LUND UNIVERSITY

Investigation of Partially Premixed Combustion in an Optical Engine

In-Cylinder Flow and Combustion Characterization

Tanov, Slavey

2017

Document Version:
Publisher's PDF, also known as Version of record

Link to publication

Citation for published version (APA):
Tanov, S. (2017). *Investigation of Partially Premixed Combustion in an Optical Engine: In-Cylinder Flow and Combustion Characterization*. [Doctoral Thesis (compilation), Combustion Engines]. Energy Sciences, Lund University.

Total number of authors:
1

General rights
Unless other specific re-use rights are stated the following general rights apply:
Copyright and moral rights for the publications made accessible in the public portal are retained by the authors and/or other copyright owners and it is a condition of accessing publications that users recognise and abide by the legal requirements associated with these rights.
• Users may download and print one copy of any publication from the public portal for the purpose of private study or research.
• You may not further distribute the material or use it for any profit-making activity or commercial gain
• You may freely distribute the URL identifying the publication in the public portal

Read more about Creative commons licenses: https://creativecommons.org/licenses/

Take down policy
If you believe that this document breaches copyright please contact us providing details, and we will remove access to the work immediately and investigate your claim.

LUND UNIVERSITY

PO Box 117
221 00 Lund
+46 46-222 00 00

Investigation of Partially Premixed Combustion in an Optical Engine

Investigation of Partially Premixed Combustion in an Optical Engine

In-Cylinder Flow and Combustion Characterization

by Slavey Tanov

LUND
UNIVERSITY

Doctoral Thesis

Thesis advisor: Professor Öivind Andersson
Faculty opponent: Professor Fabrice Foucher, Université d'Orléans, France

To be presented, with the permission of the Faculty of Combustion Engines of Lund University, for public criticism in the M:B lecture hall at the Department of Energy Sciences on Friday, the 16th of June 2017 at 10:15.

Organization	Document name
LUND UNIVERSITY Department of Energy Sciences Box 188 SE–221 00 LUND Sweden	**DOCTORAL DISSERTATION** Date of disputation 2017-06-16 Sponsoring organization
Author(s) Slavey Tanov	

Title and subtitle

Investigation of Partially Premixed Combustion in an Optical Engine: In-Cylinder Flow and Combustion Characterization

Abstract

The diesel engine is one of the most economic power sources and is therefore used in a range of technical solutions. The low fuel consumption combined with high engine performance makes it attractive for transportation vehicles. They are relatively unproblematic in terms of emissions of carbon-monoxide and hydrocarbons but, on the other hand, they are associated with high emissions of nitrogen oxides and soot. In the atmosphere, these emissions constitute a serious concern for both human health and the environment. For this reason, the recent research and development efforts of many automakers and research institutes have shifted focus to new technologies such as advanced combustion concepts. Partially premixed combustion (PPC) is one of the novel combustion concepts that aim to yield low NO_x and soot emissions while maintaining high engine efficiency. This combustion process belongs to a class of technologies called low temperature combustion concepts. In conventional diesel combustion, the combustion is promptly initiated by auto-ignition as fuel is injected into the cylinder, vaporizes, mixes, and reacts with hot air. In PPC, by contrast, all the fuel is injected before it auto-ignites, which is made possible by the distribution of mixture strengths (fuel stratification) prior to combustion. The PPC process combined with high exhaust-gas recirculation (EGR) rates gives lower combustion temperatures and thus reduces the NO_x emissions and soot formation.

All the combustion occurs in premixed mode, which mainly means in mixture packets that have mixed with oxygen to different degrees during the ignition delay. The ignition delay is controlled by temperature, charge composition, fuel type and fuel injection timing. The work presented in this thesis is experimental investigations to understand the in-cylinder combustion and fuel–air mixing process under gasoline-PPC conditions. The first part describes a new approach to determine the in-cylinder combustion stratification for various injections strategies. The second part is devoted to the in-cylinder fluid motion which is important for the fuel-air mixing, heat transfer, combustion, and emission formation processes. For these two parts, an optical engine is used to carry out the experimental investigations. The last part consists of multi-cylinder experiments where the engine is fuelled with a blend between gasoline and ethanol and combustion is studied through an endoscope. Different strategies were used to maintain stable combustion and relatively low emissions of soot under PPC conditions.

Key words

PPC, In-Cylinder Flow, Gasoline, Gasoline-Ethanol, Optical Diagnostic, Multiple Injection, Stratification Level

Classification system and/or index terms (if any)

Supplementary bibliographical information	Language
	English
ISSN and key title	ISBN
	978-91-7753-344-3 (print) 978-91-7753-345-0 (pdf)
Recipient's notes	Number of pages: 228 / Price
	Security classification

I, the undersigned, being the copyright owner of the abstract of the above-mentioned dissertation, hereby grant to all reference sources the permission to publish and disseminate the abstract of the above-mentioned dissertation.

Signature _____ Date 2016-05-22

DOKUMENTDATABLAD enl SIS 61 41 21

Investigation of Partially Premixed Combustion in an Optical Engine

In-Cylinder Flow and Combustion Characterization

by Slavey Tanov

LUND
UNIVERSITY

A doctoral thesis at a university in Sweden takes either the form of a single, cohesive research study (monograph) or a summary of research papers (compilation thesis), which the doctoral student has written alone or together with one or several other author(s).

In the latter case the thesis consists of two parts. An introductory text puts the research work into context and summarizes the main points of the papers. Then, the research publications themselves are reproduced, together with a description of the individual contributions of the authors. The research papers may either have been already published or are manuscripts at various stages (in press, submitted, or in draft).

Funding information: The research leading to these results has received funding from the People Programme (Marie Curie Actions) of the European Union's Seventh Framework Programme FP7/2007-2013/ under REA grant agreement n° 607214.

© Slavey Tanov 2017

Faculty of Combustion Engines, Department of Energy Sciences

ISBN: 978-91-7753-344-3 (print)
ISBN: 978-91-7753-345-0 (pdf)
ISSN: <0282-1990>

Printed in Sweden by Media-Tryck, Lund University, Lund 2017

Tief verbunden und dankbar bin ich meinen Eltern und meinen Bruder für die unermüdliche Unterstützung bei der Erstellung dieser Doktorarbeit.

Abstract

Due to the strong focus on emission reduction and improving fuel economy in the transport sector, many researchers explore and develop various advanced combustion strategies. Partially premixed combustion (PPC) is a novel strategy to face these major challenges, which has received increased attention. The goal of the PPC process is to achieve sufficient pre-mixing between the fuel and air to avoid soot formation, and to maintain combustion temperatures low enough to reduce thermal NO_x formation by using high EGR rates. Due to its potential to simultaneously reduce soot and NO_x, PPC may reduce the demand on exhaust aftertreatment systems in motorized vehicles. Stratification of both the charge and temperature are important for achieving PPC. They can be achieved by advancing the fuel injection into the cylinder, and by controlling the composition of the fuel-air mixture to promote auto-ignition. In terms of stratification levels, PPC ranges between the fully homogeneous (less stratified) HCCI concept and the conventional diesel combustion (highly stratified). By utilizing proper fuel injection and dilution strategies, the combustion is controlled so that excessive heat-release rates can be avoided. The work presented in this thesis are experimental investigations of the in-cylinder combustion and fuel–air mixing processes under PPC conditions. The objective is to gain information and better understanding of how the combustion stratification level and the in-cylinder turbulent flow fields affect combustion and emission formation. The last stage of the research mainly focused on the detailed study of different EGR settings at various air-fuel ratios to characterize the gasoline PPC concept.

Using split injections has the advantages of reducing the maximum heat release rate, thus reducing the combustion noise, as well as extending the operable range. On the other hand, split injections can lead to increased *UHC* and *CO* emissions. Multiple injection strategies also provide flexibility concerning the fuel stratification, which is used in this thesis to extend the ignition delay for enhanced fuel-air mixing prior to the start of combustion.

In the first measurements, OH* chemiluminescence was imaged in the cylinder of an optical engine to study the combustion process throughout the cycle and to analyze the degree of stratification. Hot residual gases were trapped by using NVO to dilute the cylinder mixture. The results clarify the mechanisms controlling the PPC energy release. Chemiluminescence imaging shows that PPC features a high temperature reaction zone that appears to grow by the appearance of small auto-ignition regions. The rate of reaction zone growth is controlled by the stratification level. Going from single injections to a triple injection strategy, a distinct change in the stratification is seen, which is also apparent in the heat release rate.

Turbulent flow structures within the cylinder are essential to the mixture preparation, combustion, and pollutant formation in light-duty (LD) direct-injection diesel engines. Both

the mean flow and the turbulence significantly impact the fuel stratification in combustion systems with pre-mixed charge. In this second stage of the research, the in-cylinder flow is characterized by particle imaging velocimetry (PIV). This technique is used to explain how multiple injection strategies affect the flow pattern, turbulence and cyclic variation within the piston bowl. The PIV method enables bulk flow analysis during the compression, injection, combustion, and expansion phases. The flow field is recorded in a vertical section through the squish region and the piston bowl.

The last part in this thesis deals with multi-cylinder engine experiments focusing on strategies to operate the engine with high RON fuels (RON 98) using the PPC approach. Various strategies were applied to maintain LTC conditions with stable combustion (COV of IMEP less than 3 percent), low combustion noise, and relatively low emissions of soot. The fuel used was E30, which is gasoline with 30 percent ethanol. It was shown that using a double injection strategy at an engine speed of 1000 rpm, this fuel performs reasonably well up to an engine load of 8 bar IMEP. The combustion phasing was kept constant at 4° aTDC (±1°). This was done to maintain relatively low combustion noise and to sustain combustion at highly diluted conditions (30 percent EGR). In addition to engine and emissions data, endoscope images were acquired using an AVL VisoScope to monitor the effect of given parameters on natural combustion luminosity.

Populärvetenskaplig sammanfattning på svenska

Dieselmotorn är en den mest ekonomiskt fördelaktiga kraftkällan och används i många tekniska applikationer. Kombinationen av låg bränsleförbrukning och hög prestanda gör den attraktiv som drivkälla i transportfordon. Dessutom är dieselmotorns utsläpp av kolmonoxid och kolväte låga. Däremot har den höga utsläpp av både sot och kväveoxider luftföroreningar som både skadar människors hälsa och påverkar miljön negativt. På grund av detta har fordonstillverkare och forskningsinstitut inriktat forskningen mot nya, avancerade förbränningskoncept. Ett av dessa är partiellt förblandad förbränning (eng partially premixed combustion, PPC). Målet med detta förbränningskoncept är att kraftigt reducera utsläppen av både sot och kväveoxider men samtidigt uppnå en hög verkningsgrad. PPC konceptet utgör en del av förbränningstypen som kallas för lågtemperaturförbränning. Förbränningen i en konventionell dieselmotor injiceras bränslet in i den heta, komprimerade luften i cylindern. Medans bränslet injiceras i luften förångas den och blandas med luften för att sedan förbrännas. Förbränningen sker alltså medans insprutningen pågår. I PPC-konceptet däremot startar förbränningen efter att injiceringen av bränsle i cylindern har avslutats. Hur lång fördröjningen är mellan slutet av bränsleinjektionen och början av förbränningen (=tändfördröjning) beror på ett flertal parametrar, såsom temperaturen, bränslefördelningen i cylindern, bränsletyp och insprutningstidpunkt. Arbetet som presenteras i denna avhandling berör utförda experimentella undersökningar för att öka förståelsen över förbrännings- och blandningsförloppet inuti cylindern vid PPC förbränning. Den första resultatdelen beskriver ett nytt angreppsätt för att fastställa förbränningsstratifieringen i cylindern vid olika insprutningsstrategier. Den andra delen fokuserar på fluidens rörelser inuti cylindern. Detta är viktigt eftersom detta har en signifikant påverkan på värme- och bränsle/luft-blandningsprocessen, värmeöverföring, förbränningsprocessen och bildningen av avgasemissioner. Experimenten i dessa båda delar har utförts i en optisk motor. Den tredje och sista delen berör experiment utförda i en multicylinder motor som körs med en blandning av bensin och etanol. I detta fall har endoskop-teknik använts för att studera förloppet inuti cylindern. Flertalet olika strategier har provats ut för att bibehålla PPC förhållanden optimerade för stabil förbränning och relativt låga emissioner och sotbildning. Kombinationen PPC och hög andel avgasåtercirkulation reducerar förbränningstemperaturerna och därigenom minskas även kväveoxidutsläppen och sotbildningen.

List of publications

I **Combustion Stratification with Partially Premixed Combustion, PPC, Using NVO and Split Injection in a LD - Diesel Engine**

Slavey Tanov[1], Robert Collin[2], Bengt Johansson[1], Martin Tunér[1]
[1] *Division of Combustion Engines, Lund University, Sweden*
[2] *Division of Combustion Physics, Lund University, Sweden*

SAE International Journal Engines 2014-01-2677

II **Effects of Injection Strategies on Fluid Flow and Turbulence in Partially Premixed Combustion (PPC) in a Light Duty Engine**

Slavey Tanov[1], Bengt Johansson[1], Zhenkan Wang[2], Matthias Richter[2], Hua Wang[3]
[1] *Division of Combustion Engines, Lund University, Sweden*
[2] *Division of Combustion Physics, Lund University, Sweden*
[3] *Dantec Dynamics, Denmark*

SAE Technical Paper 2015-24-2455

III **High-Speed Particle Image Velocimetry Measurement of Partially Premixed Combustion (PPC) in a Light Duty Engine for Different Injection Strategies**

Zhenkan Wang[2], Slavey Tanov[1], Bengt Johansson[1], Matthias Richter[2], Marcus Aldén[2], Hua Wang[3]
[1] *Division of Combustion Engines, Lund University, Sweden*
[2] *Division of Combustion Physics, Lund University, Sweden*
[3] *Dantec Dynamics, Denmark*

SAE Technical Paper 2015-24-2454

IV **Analyzing of In-Cylinder Flow Structures and Cyclic Variations of Partially Premix Combustion in a Light Duty Engine**

Slavey Tanov[1], Bengt Johansson[1], Mohammad Izadi Najafabadi [2], Hua Wang[3]
[1] *Division of Combustion Engines, Lund University, Sweden*
[2] *Division of Combustion Technology, Eindhoven University of Technology, Netherlands*
[3] *Dantec Dynamics, Denmark*

FISITA Conference Paper F2016-ESYF-005

v **Effects of Injection Timing on Fluid Flow Characteristics of Partially Premixed Combustion Based on High-Speed Particle Image Velocimetry**

Mohammad Izadi Najafabadi[1], Bart Somers[1], Slavey Tanov[2], Bengt Johansson[2], Hua Wang[3]
[1] *Division of Combustion Technology, Eindhoven University of Technology, Netherlands*
[2] *Division of Combustion Engines, Lund University, Sweden*
[3] *Dantec Dynamics, Denmark*

SAE International Journal Engines 2017-01-0744

vi **Influence of Spatial and Temporal Distribution of Turbulent Kinetic Energy on Partially Premixed Combustion Heat Transfer in a Light Duty**

Slavey Tanov[1], Öivind Anderson[1], Leonardo Pachano2[2], Antonio García[2], José M. García-Oliver[2], Zhenkan Wang[3],Matthias Richter[2], Marcus Aldén[2], Hua Wang[4]
[1] *Division of Combustion Engines, Lund University, Sweden*
[2] *CMT Motores Térmicos – Universitat Politècnica de València, Spain*
[3] *Division of Combustion Physics, Lund University, Sweden*
[3] *Dantec Dynamics, Denmark*

Manuscript submitted to Applied Thermal Engineering, *ATE* − 2017 − 2876.

vii **Combustion and Emission Characteristics of Gasoline-PPC with small quantities of Ethanol**

Slavey Tanov[1], Öivind Anderson[1], Khanh Cung[2], Stephen Ciatti[2]
[1] *Division of Combustion Engines, Lund University, Sweden*
[2] *Argonne National Laboratory, USA*

To be submitted to a journal

All papers are reproduced with permission of their respective publishers.

Acknowledgements

As my time at Lund University is near the end, I would like to express my gratitude to my main supervisors Bengt Johansson and Öivind Andersson for all the support and help. In 2013 the journey as a PhD student started with Bengt. Thank you for welcoming me at the Combustion Engines department with an interesting project and many good ideas, great supervision and support but also for taking your time for any discussion when needed. His knowledge about thermodynamics and combustion engines is truly impressive. I would like to learn more from Bengt, however he has chosen for some reason being close to the equator. In 2016, I had the pleasure to be a student of Öivind Andersson. I am equally thankful for his constant guidance and tireless support for the past 1.5 years. Especially for his intensively support in planning experiments and thesis writing. Thank you both!

I would like to thank my co-supervisor Per Tunestål for all the good advice during these years. He was always helpful and had useful answers related to combustion engines, Matlab, culture, language and Malmö FF. Every discussion with him was an enrichment. At the same time, I am grateful to Martin Tuner for having many interesting and valuable discussions.

I am grateful to Hua Wang from Dantec Dynamics for his extraordinary skills in the field of fluid dynamic and great support with the laser diagnostic setup. His great introduction and help in applying PIV technique grants my profound admiration.

Thanks also to the gentlemen from the workshop for maintaining our labs. Without the help of the technicians, it would be not easy to have well-working research engine.

I had the opportunity and chance to visit two different engine test facilities: Argonne National Labs in Illinois, and TU Eindhoven in Netherlands. I am very grateful to all the persons who made the visits as a guest researcher possible. Both places were an excessive personal enrichment where I had the chance to meet great engineers and persons. A distinct thanks to the ANL team with Stephen Ciatti, Khanh Cung and Tim Rutter for their hospitality and support. With their help, it was possible to complete the experiments in time before the end of my stay, and we managed it. At the same time, I want to stress out the same hospitality and support from team Eindhoven. It was a pleasure to work with Bart Somers and Mohammad (nick name Mo) Izadi. Apart from the countless time in the engine lab, it was always a real fun to hang out with Mo. I also want to thank to the colleagues from Combustion Physics. Most notably I enjoyed the great time with Zhenkan Wang. His precision work and ease of mind is highly admirable. I truly liked the numerous discussions with him across all the different topics, be it about hair stylist or laser techniques. Thank you for your great contribution in this work.

I was also very lucky to have such friendly and helpful colleagues at the Combustion Engine

Division. Therefore, I am grateful for all the good times and numerous conversations during “fikka”. In particular, I want to thank for Guillaume (spelling: Giom) Lequien, Pablo Garcia, Nhut Lam, Prakash Narayanan, Marcus Lundgren, Lianhao Lin and Tianhao Yang.

Finally, I want to thank my parents and brother for being be a great source of inspiration and support throughout my live. Special thanks to my brother, who just taught me everything, cannot simply imagine having a better brother then you!

Nomenclature

aTDC	-	After Top Dead Center
bDC	-	Bottom Dead Center
CA10	-	Crank Angle degree at 10% heat release completion
CA50	-	Crank Angle degree at 50% heat release completion
CAD	-	Crank Angle Degree
CCD	-	Charge-coupled device
CDC	-	Conventional Diesel Combustion
CFD	-	Computational Fluid Dynamics
CI	-	Compression Ignition
CN	-	Cetane number
CO	-	Carbon monoxide
CO_2	-	Carbon dioxide
COV	-	Coefficient of variation
DI	-	Direct Injected
DPF	-	Diesel particulate filter
EGR	-	Exhaust Gas Recirculation
EOI	-	End Of Injection
EU	-	European Union
FSN	-	Filtered Smoke Number
GDCI	-	Gasoline Direct Injection Compression Ignition
GCI	-	Gasoline compression ignition
h	-	Heat transfer coefficient
HCCI	-	Homogeneous charge compression ignition
IA	-	Interrogation area
ICE	-	Internal Combustion Engine
ID	-	Ignition Delay
IMEP	-	Indicated Mean Effective Pressure
IMEPg	-	Gross Indicated Mean Effective Pressure
LIF	-	Laser Induced Fluorescence
LNT	-	Lean NOx trap
LTC	-	Low Temperature Combustion
MK	-	Modulated Kinetics
MK1	-	Environmental Class 1 Swedish diesel
NOx	-	Nitrogen Oxides
OH	-	Hydroxyl radical
p	-	Pressure
PCA	-	Priciple component analysis
PFI	-	Port fuel injection
PCCI	-	Premixed charge compression ignition

PIV	-	Particle image velocimetry
PLIF	-	Planar Laser Induced Fluorescence
PM	-	Particulate Matter
POD	-	Proper orthogonal decomposition
PPC	-	Partially Premixed Combustion
PRF	-	Primary Reference Fuel
PRF70	-	PRF with 70% iso-octane and 13% *n*-heptane
RCCI	-	Reactivity Controlled Compression Ignition
RON	-	Research octane number
Rs	-	Swirl ratio
SCR	-	Selective Catalytic Reduction
SI	-	Spark ignition
SOC	-	Start of combustion
SOI	-	Start Of Injection
T	-	Temperature
TDC	-	Top Dead Center
TiO_2	-	Titanium oxide
TKE	-	Turbulent kinetic energy
UHC / HC	-	Unburned Hydro Carbons
UNIBUS	-	Uniform Bulky combustion System
λ	-	Air-fuel equivalence ratio
ϕ	-	Fuel-air equivalence ratio

Contents

CHAPTER 1

INTRODUCTION

1.1 Background and Motivation

A steady growth of worlds population and increased living standards are responsible for a continuously increase in energy demand. The today's global energy conversion through combustion covers 91% [1], thereby the internal combustion engine (ICE) plays an important role. In the past century the ICE has spread worldwide as a propulsion unit for land and water vehicles, but also as a stationary unit for the propulsion of work machines and generators. In fact, the ICE is ultimately enabling today's mobility and the chemical combustion of liquid fuel is the primary energy source used in the transportation sector. This sector is still dominated by two engine types: First is the "Otto" engine presented by Nicolaus Otto in 1876 and second goes to Rudolph Diesel who invented the first compression ignition engine in 1892.

The passenger and commercial vehicles are predominantly operated by both, otto and diesel engines, thus the transported volume of goods and material parts are primarily delivered by diesel engines. To illustrate the meaning of ICE Figure 1.1 shows the energy use in EU with different sectors (nuclear, renewables, gas, coal, and petroleum production). A significant amount from the petroleum production is used for the transportation sector. Another important aspect that can be drawn from this chart is the uneven ratio of used energy (1/3) to energy losses (2/3). Even when the energy loss in combustion engines are high, the engine still remains as a reliable energy conversion device that converts chemical potential into useful work through combustion.

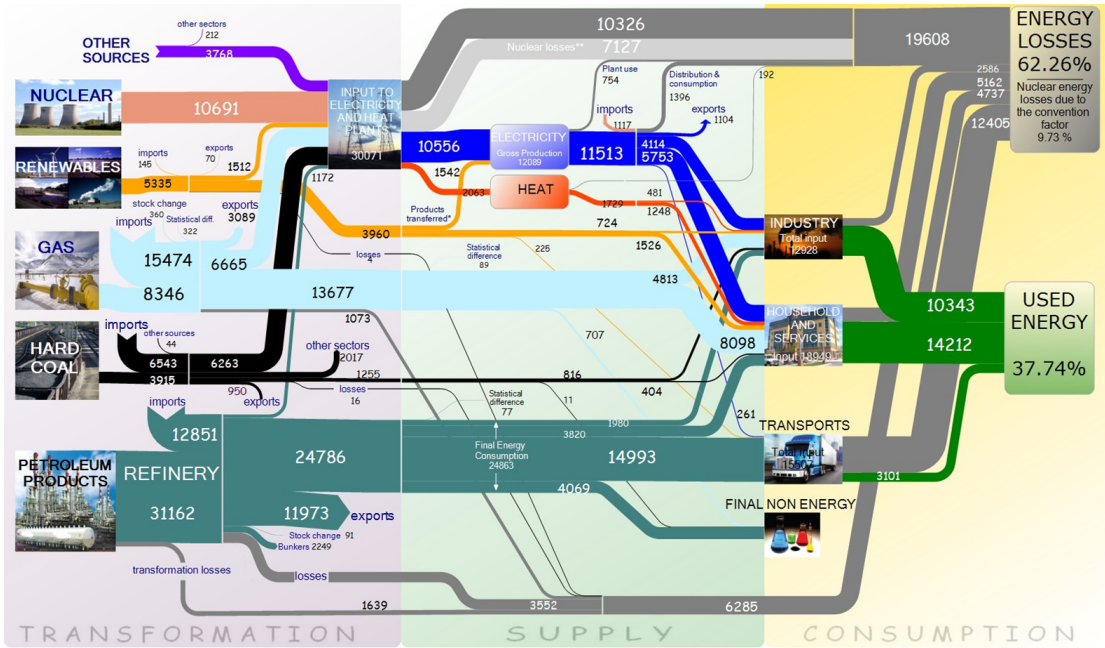

Figure 1.1: EU-27 Energy flow trends shows the energy conversion from primary energy (coal, oil, natural gas, etc) to secondary energy commodities such as electricity, heat, ect. The right hand side of the diagram shows the final mix of energy consumption by different energy users (including: industry, domestic,transport other final consumers and non-energy use). Reproduced from [2].

Regardless of the engine design or type of fuel, the transport sector has huge impact on the greenhouse effect by polluting CO_2 exhaust emissions [3]. This is a non-toxic and naturally occurring gas in our atmosphere, but through the excessive combustion of fossil fuels the concentration increases, consequently causing global warming. The phenomena occurs as sunlight passes trough our atmosphere and heats the earths surface. When sunlight is reflected, the greenhouse gases absorbs the heat and the energy is scattered in the atmosphere, consequently heating earth [4].

For this reason, a great deal of effort is being devoted to reducing emissions from combustion engine, which first appeared by the state of California in 1959 as a consequence of the smog problems in Los Angeles. In the 1960's, the first legislation was set in California [5]. In the later years Europe, US and Japan were setting first legislative steps towards reduction of the vehicle air pollution and the car manufactures have to meet the emission standards. In 1993 European Union introduced Euro I emission standards for passenger cars and light trucks (also known as EC 93) [5]. The legislated emissions are carbon monoxide (CO), unburned hydro carbons (UHC), nitrogen oxides (NO_X) and particulate matter (PM). Since January 2014 the new stricter Euro 6 regulations came into force and are mandatory for all new manufactured vehicles in Europe. Euro 6 emissions standard is relatively uncomplic-

ated for spark ignition (SI) engines. One big advantage which comes with the SI engines is the three-way after treatment system which enables sufficient emission reduction for stoichiometric (λ=1) combustion. For diesel engines though, it is much more challenging and complicated to introduce simple after treatment systems since they overall operate under lean ($\lambda > 1$)conditions.

Therefore the legislated emissions for diesel engines are as following: Particulate matter (*PM*), nitrogen oxides (NO_X), unburned hydro carbons (*UHC*) and carbon monoxide (*CO*). Under conventional diesel condition, the combustion pass through both rich – and lean fuel regions forming soot and NO_X respectively. Particulate matter (*PM*, also referred to as soot) are strong functions of equivalence ratio and temperature (diffusion combustion). In Order to reduce *PM* and NO_X effectively expensive and fuel consumption devises are essential in the exhaust line. Diesel particulate filter (DPF) is widely used tool in diesel engines to reduce the *PM* accumulation. However, DPF requires periodic regeneration for removal of the collected *PM*, which often requires additional fuel injections during the expansion stroke and though linked with higher fuel consumption.

Conversely, to decrease NO_X emissions catalytic devices like selective catalytic reduction (SCR) or lean NO_X traps (LNT) can be used. Thus, SCR technology requires the introduction of urea, which is injected at small rates via an additional injector into the exhaust system. However, installation of such after treatment systems (DPF and SCR) coupled with additional need of fuel are forcing combustion researcher for reducing of *PM* and NO_X emissions within the cylinder.

To overcome the well-known diesel trade-off recent research has led to develop several non-traditional combustion concepts. Many of this alternative combustion concepts enable the unique feature to simultaneously reduce exhaust emissions within the combustion chamber and on other hand maintain high thermal efficiencies. Accordingly, Partially Premixed Combustion (PPC) is one of the promising LTC pathway, which is studied in this thesis.

1.2 Research objective

The objective of this thesis is to gain further knowledge about PPC concept with a basic physical understanding of the underlying combustion and flow processes that occur in a direct injection light-duty engine. The aim of this study was to explore the combustion stratification and the mechanisms of turbulent bulk flow structure which plays a dominant role in mixture preparation and the subsequence combustion process related to PPC engine combustion.

Unlike conventional compression ignition, PPC relies on high exhaust gas recirculation (EGR) levels and enhanced mixing duration to achieve sufficient mixing between fuel and

air prior the autoignition. Therefore, an important part of the project was to understand and describe the various flow structures and turbulence generation mechanisms observed in the engine. This structures are not only responsible for ensuring that fuel and fresh air are transported to the same location and mixed within the cylinder, but also for generating intense turbulence before cylinder volume expansion.

Another distinguish feature of PPC compared to other strategies is the importance of fuel stratification to control the combustion. It is not desired to have a fully premixed mixture which leads to aggressive and uncontrolled combustion characteristics. On other hand, high stratification lead to diesel-like combustion process and hence to the typical emission issues. PPC, with a moderate stratification, is located between those to combustion processes. Therefore, great effort was spent to create a better understanding on the combustion process and on determining the stratification level related to PPC concept.

1.3 Method

This work involves an experimental approach based on optically studies in order to the investigate the PPC concept. An effective way for detailed examination of in-cylinder process is to use advanced laser diagnostic techniques to answer research questions related to flow characteristics, fuel stratification and fuel distribution. A fairly good understanding of the in-cylinder state is obtained by simultaneously recording of the cylinder pressure trace and laser-based diagnostics. By performing both measurement techniques, the indicated pressure traces are used to correlate to the 2D combustion or flow imaging data. The indicated pressure sampling contains information about combustion phasing, combustion duration and engine load; while the optically results give a general and detailed information about the in-cylinder combustion and flow characteristics.

CHAPTER 2

ADVANCED COMBUSTION CONCEPTS

2.1 Conventional Diesel Combustion

It is well known that the conventional diesel engine offers better efficiency compared to SI engines due to its high compression ratio and lack of throttling losses. The combustion process of diesel engines is highly complex and is characterized by heterogeneous mixture formation and combustion. Liquid fuel is injected into the combustion chamber under high pressure, usually close to top dead center (TDC). The injected fuel enters the combustion chamber at high velocities and atomizes into small droplets, vaporizes and mixes with air and trapped exhaust gases (internal or external EGR), resulting in a heterogeneous mixture of fuel and air [6]. As seen in Figure 2.1, which shows a typical heat release curve from a diesel engine, there is only a limited time available for mixture formation between the start of injection (SOI) and start of combustion (SOC). Combustion is initiated after a short delay by the high pressure and temperatures trough a spontaneous auto-ignition process of the air-fuel mixture, hence the name compression ignition (CI). This leads to a rapid combustion rate of the mixture with a steep heat release gradient in a typical manner of a premixed combustion. While the injection is progressing after the premixed combustion, a lifted flame is established and fuel burns in diffusion combustion at the edge of the spray. This phase is also often referred as spray driven combustion. Once the injection ends, the late mixing-controlled combustion takes place and where the remaining fuel burns slowly away. The initiated heat release rate is illustrated with its temporal phases in Figure 2.1.

The heat release shows the different phases of combustion as a function of time, but it gives no spatial information about the combustion process. Another widely used representation

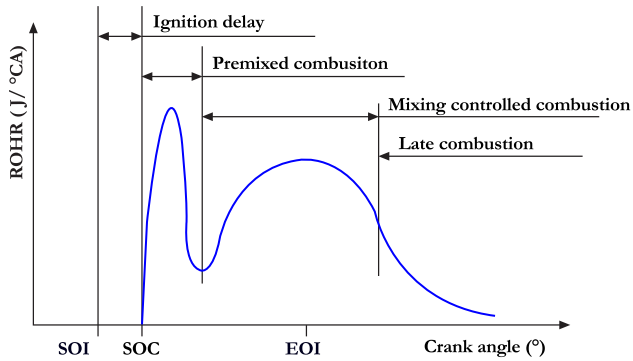

Figure 2.1: Schematic heat release rate as function of crank-angle in degree for conventional diesel combustion (CDC) identifying different CDC phases.

of diesel combustion is the conceptional model from Dec [7]. This model is based on experimental results from planar laser measurements conducted in an optical engine and describes the quasi-steady diesel jet.

The conceptual model in Figure 2.2 shows the development of a single diesel fuel jet, which contains several zones. On the left side of the image, liquid fuel penetrates into the combustion chamber (injected trough a nozzle), mixes with the hot ambient charge during the characteristic 'liquid length' and fuel begins to vaporize. The spray reaches its maximum liquid length. Beyond this point only vaporized fuel-air mixture is present and continues to enter the hot gases. Auto-ignition occurs in the subsequent fuel-rich mixture zone where it undergoes premixed combustion, where first poly-aromatic hydrocarbons (PAH) start to form [8, 9]. This are presources of soot and initiate the formation of soot particles inside the spray. Further downstream in the jet, the soot particles grow in size and concentration inside the diffusion flame due to lack of oxygen. On the outer reaction zone of the diffusion flame, NO_X production occurs due to near stoichiometric conditions and high ambient temperature.

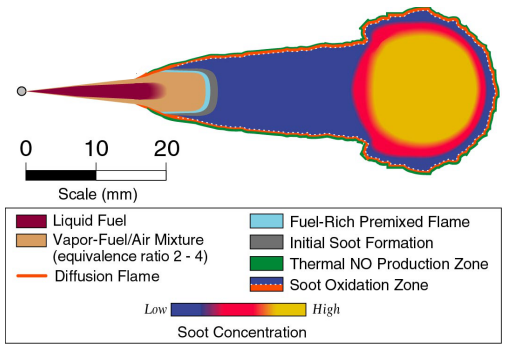

Figure 2.2: Schematics of Dec's conceptual model during the quasi-steady period of diesel combustion. Reproduced from [7].

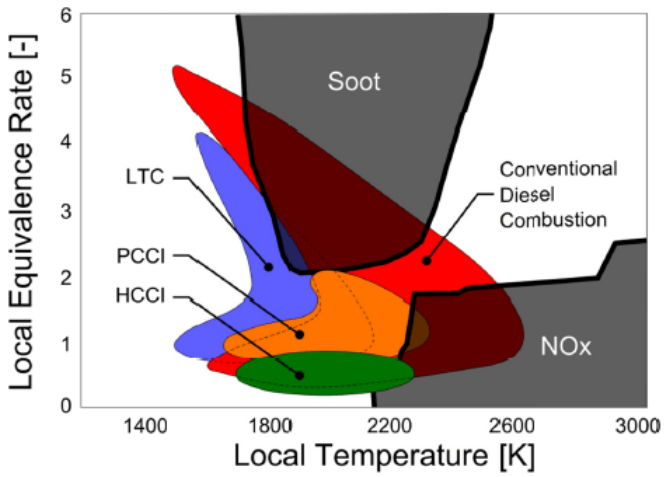

Figure 2.3: Illustration of different operating regimes for: CDC, LTC, PCCI and HCCI on a Φ-T map together with soot and NO_X islands. Reproduced from [10].

A useful picture to illustrate the trade-off between soot and NO_X emission for conventional diesel combustion is presented in Figure 2.3. Kamimoto and Bae [11, 12] proposed first a ϕ-T diagram in order to visualize the link between in-cylinder conditions with the regions where pollutant formation occurs. They combined and plotted a soot island, obtained from gas sampling data and literature data, and NO_X island, determined by Zeldovich mechanisim, in the ϕ-T space. As can be seen, this Figure 2.3 shows that the diesel combustion process encompasses both the soot and a NO_X islands during a combustion cycle. Neely *et al.* [13] later overlaid many combustion concepts in ϕ-T space to demonstrate that a simultaneously reduction of these two pollutants can be achieved increasing ignition delay

in combination, such that the peak equivalence ratio is below the soot formation threshold. On the other hand, high EGR rate often lead to a reduction of oxygen concentration and subsequently to lower flame temperatures. This topic is further discussed in chapter 2.2.

2.1.1 Turbulent flow structure in direct injection light duty engine

Swirl and Tumble flow

One of the central tasks of engine development is indicated by the in-cylinder turbulent flow and has a great importance in the mixture preparation, combustion and pollutant formation process in direct injection diesel engines [6]. In general, the airflow in engines are basically characterized by swirl or tumble motion. Figure 2.4 illustrates both, swirl motion which corresponds to the global rotation of the fluid around the axial direction of the cylinder, while tumble motion describes general flow around horizontal axis. Swirl is generated by the engine intake system to give a tangential component to the intake flow as it enters the cylinder. Additionally, it greatly enhances the mixing of air and fuel to achieve a combustable mixture in the very short time. On other hand, tumble motion brakes down during the compression stroke. The corresponding vortical structures are broken into small eddies which enhance the overall level of turbulence. Several studies, both have been conducted in order to understand the resulting flow configuration at the end of the compression stroke [14, 15].

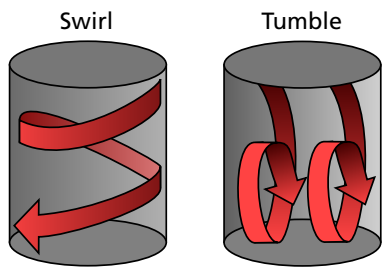

Figure 2.4: Swirl and tumble motion in an engine cylinder. Image from [16].

The control of fluid flow within the cylinder of IC engines is achieved primarily trough the design of induction port and valve geometries, cylinder head and piston crown geometry. The concern of generating a large scale swirl motion in diesel engines plays an important role, because momentum and energy stored in this rotational motion can survive for a longer time in the cylinder and have a chance to affect combustion when the inlet valves are closed.

2.1.2 Squish-swirl interaction

As the process of compressing the swirling motion into the bowl, particular flow structures are generated because of the rearrangement of the in-cylinder angular momentum by the squish flow [17, 18]. If the piston and combustion chamber have been designed to produce squish, then the fluid squeezed out of the squish volume produces an organized flow, which breaks up into turbulence. Another effect of the squish flow is, that it has a dynamical effect on the organized swirl flow [14]. Prior to TDC, these flows (squish and swirl) supplies the fuel-air mixing process, through bulk transport by the mean flow and intense turbulence as well as trough the small-scale mixing by the turbulent eddies. Last one subsequently allows molecular diffusion to rapidly mixing of fuel and air on a molecular level and their lifetime is much shorter than the time for induction and compression [17].

The bulk flow structures are also equally important during expansion cycle, hence the oxidation of unburned fuel and particulates is limited by mixing rate. In this phase, the bulk flow structures are responsible for ensuring that fuel and fresh oxidants are transported to the same location within the cylinder. Furthermore, they are also responsible for generating the intense turbulence required to obtain small-scale mixing before falling temperatures due to cylinder volume expansion and ongoing slow chemical reactions excessively [19].

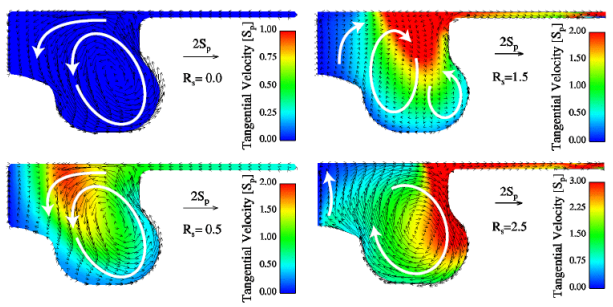

Figure 2.5: Illustration of vertical flow structures by the squish-swirl interaction at various levels of swirl. Reproduced from [20].

Miles *et al.* [20] investigated the interaction process of squish-swirl based on flow swirl level or swirl ratio (Rs). The numerical results presented in Figure 2.5 illustrate the vector fields for different Rs at TDC position. As can be seen, for low swirl ratio (Rs=0), the squish flow penetrates to nearly the cylinder centreline before it turns down into the bowl, as required by symmetry constraints. As the swirl ratio is increased, the inward penetration of the squish flow is reduced. For high swirl levels, the centrifugal forces are sufficiently great that the squish flow turns down into the bowl as soon as the combustion chamber geometry permits. Note that the direction of rotation of the vortex structure that dominates the bowl at Rs=0 and at Rs=.5 has been reversed.

2.1.3 Spray-swirl interaction

Another important contribution by Miles *et al.* [21, 22, 23] was the investigation of fuel injection process on the flow structures and interactions with the three dimensional swirl motion.

As depicted in Figure 2.6, for low swirl ratios a single vortex structure deep in the bowl was formed by the deflection of the fuel jet at the bowl wall. This structure transports high angular momentum fluid from near the bowl rim down into the bowl, where it is redirected at the bowl pip inward to the central bowl. Although the tangential velocity (scalar plot) of this fluid increases as it moves inward, the centrifugal forces are sufficiently small that they do not strongly alter the vortex structure. On the contrary, a double vortex structure for higher swirl ratios has formed as a result of larger centrifugal forces associated with the higher angular momentum. The inwardly displaced fluid from squish region is forced to return to the outer regions of the bowl, where a small counter-clockwise vortex is depicted. Moreover, a clockwise-rotating vortex becomes progressively smaller and is centred lower within the bowl, and a complementary counter-rotating vortex forms in the upper central region of the combustion chamber. The relative sizes of these vortical structures can also be impacted by injection pressure. High injection pressure increases the momentum in the fuel-induced vortex structure, thereby allowing greater inward and upward displacement of a fluid element before the vortex momentum is overcome by centrifugal forces. Hence, the size of the lower vortex increases. However, for low injection pressures this vortex is locally deeper within the bowl.

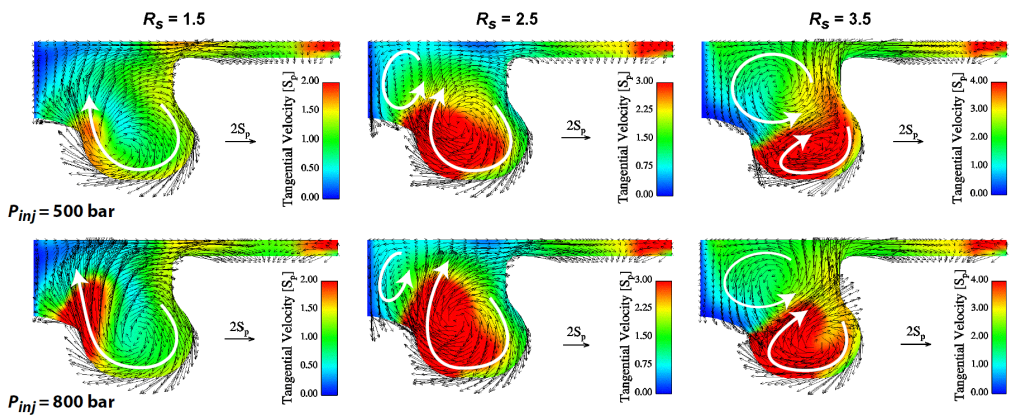

Figure 2.6: Illustration of vertical flow structures by the spray-swirl interaction at various injection pressure and swirl ratio. Reproduced from [23].

2.2 Low Temperature Combustion (LTC)

Over the past few decades, different combustion regimes in internal combustion engines have been investigated, as well as extensive research has focused on "new" hybrid form of these. The forcing idea behind developing advanced combustion concepts is driven by the diesel dilemma and have received considerable attention. The main motivation of these new alternative concepts is to reduce simultaneously NO_X and soot emission, while increasing the engine efficiency. Low NO_X emissions are achieved through minimization of peak temperatures during the combustion process. Concurrently, soot formation is inhibited due to a combination of low combustion temperatures and extensive fuel-air premixing [24].

An overall classification of the different combustion regimes are shown in a triangular diagram, Figure 2.7. Located at the top right corner is the diffusive combustion (CDC), where fuel (minimum resistance to auto-ignition) and air are first not premixed. Generally the diffusion combustion is a two stage process, where they mix in a first step (physical process) and react in the second (chemical) step, whereby the chemical process proceeds much quicker than the physical process, see section 2.1. In contrast, the upper left corner in the triangle represents the combustion process driven by the flame front propagation. In this case the fuel (high resistance to auto-ignition) and oxidant are ideally mixed and the combustion occurs when (starting from an ignition source) a flame front advances spatially through the mixture. In essence, this combustion concept is widely used in spark ignition (SI) engines. At the third corner of the triangle a combustion process is located, which should be strictly differentiated from the homogeneous flame front combustion. This concept relies on achieving a homogeneous air-fuel (any fuel with different properties) mixture prior to be auto-ignited with out a continuous flame front, consequently the combustion rate is kinetically controlled. Many researches haven shown that chemical kinetic controlled combustion can be adapted in almost all internal combustion engines, speaking SI and CI.

The transition from kinetically controlled combustion towards stratified diffusion driven combustion is shown at bottom in Figure 2.7. The images illustrates the fuel distribution prior start of combustion. As can be seen, HCCI auto-ignition differs from that of conventional compression ignition engines as it does not occur at a specific place in the spray. In between appears the PPC concept, which is neither chemically controlled nor entirely diffusion driven combustion.

Several researchers have continued to study further advanced combustion concepts which are located between each corner point of the combustion concepts triangle. An alternative concept which appears between flame propagation and kinetic controlled combustion is the so called spark assisted compression ignition (SACI). SACI relies generally that a spark initiates a propagating flame that consumes a portion of the charge and releases some of

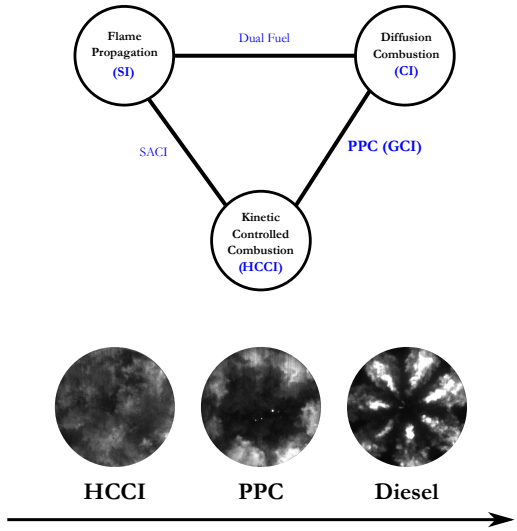

Figure 2.7: Top: Sketch of a triangular which categorizes the fundamental combustion processes in flame propagation, diffusion and kinetic controlled combustion expressed as the corner points. A related combustion mode is located between the three combustion types.
Bottom Fuel-LIF images representing the fuel distribution for the transition from HCCI-PPC-CDC.

the fuel energy. The heat released by the flame propagation increases the temperature of the remaining charge and drives it to auto-ignition. This intermediate concept where the spark influences auto- ignition was widely studied by various resarcher [25, 26, 27, 28, 29]. They have shown the capabilities of this method to improve the combustion stability, cycle to cycle control and extending the operating range.

The next concept is the combination of both flame propagation and diffusion combustion. This combustion strategy is referred as the dual fuel concept, in which the combustion starts with spray driven combustion (direct diesel injection) that ignites the homogeneous or lean charge with following flame propagation as in SI engines. There are various combinations of dual fuel concepts and they are widely used in stationary or marine application.

The third line on the triangle presents the partially premixed combustion (PPC) or gasoline compression ignition GCI. PPC can be considered as an intermediate process between the fully mixed HCCI concept and conventional spray and diffusion controlled compression ignition (diesel) combustion. For purposes of this investigations, the most important premixed LTC strategies will be discussed in the following subsection.

2.2.1 HCCI

The first category comprises strategies that falls within the often termed homogeneous-charge compression ignition (HCCI) or highly premixed combustion (HPC) with very early direct-injection. The vaporized fuel is well mixed with the charge gas in a basically homogeneous mixture prior to ignition, and is everywhere fuel-lean in the combustion chamber. As it was previously presented in Figure 2.3, HCCI can be graphically represented in the ϕ - T space at relatively constant equivalence ratio (just below ϕ=1). Typically for HCCI operation is the very early fuel injection in the compression stroke when local temperature and density are low. The uniform premixed mixture is compressed and the auto-ignition is initiated when the fuel-air charge has reached the required reactivity conditions around one or more ignition centres or "hot spots". The release of the chemical energy for HCCI during an engine cycle for a given volume of in-cylinder charge occurs very rapidly and within a narrow combustion duration, see Figure 2.8. This rapid bulk combustion arises almost simultaneously in the chamber, by avoiding the formation of a high temperature flame front or diffusion flame. The bulk combustion of a lean and diluted mixture (low oxygen concentration) drastically decreases the combustion temperature to avoid entering the NO_X island, while soot formation is also suppressed by the absence of fuel rich zones (a result of uniform premixing).

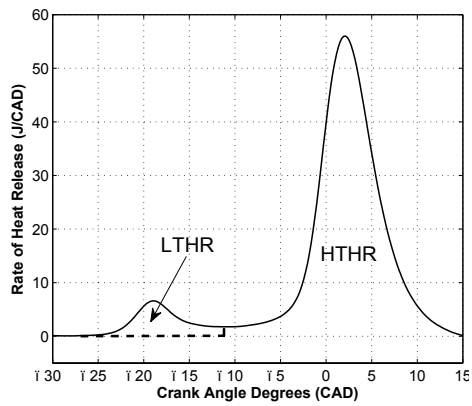

Figure 2.8: Representative heat release rate for HCCI operation.Represneted from [30].

The path to achieve HCCI operation in diesel engines is greatly reported in the literature. It can be established by either fuel injection in to the intake port [31, 32] or directly into the cylinder [33, 34, 35, 36] very early during compression stroke. Apart from the potential for reducing *NOx* and soot emissions simultaneously while maintaining high efficiencies, it suffers from some important challenges:

1. Controlling the combustion phasing of HCCI is difficult, since the combustion is driven by chemical kinetic reactions.

2. Rich or near stoichiometric conditions have the anticipation of excessive knocking and so restricts HCCI conditions to medium or low loads.

3. Due to operating with to lean mixtures, the local burning temperatures can be excessive suppressed, hence can result to incomplete combustion, leading to a rise in *CO* and *HC* emissions.

In order to overcome these issues, numerous techniques of achieving HCCI have been carried out based on creating a homogeneous or relatively uniform mixture. The pioneering research on HCCI combustion was first published by Onishi *et al.* [37] to improve part-load performance of a two-stroke SI engine. Several years later, researchers [38, 39] applied the HCCI concept to four-stroke engines and found that with high intake temperatures and the use of EGR, HCCI produced comparable fuel economy to a CDC engine. Since these studies, numerous research works have been conducted on HCCI.

The most widely used technique is the early injection approach to ensure a uniform air-fuel mixture before the auto-ignition takes place simultaneously throughout the combustion chamber near top dead center. Iwabuchi *et al.* [40] studied early injection HCCI by investigating several key parameters in both experimental and CFD works. It was found that NO_X emissions were suppressed to low levels, while *CO* and *UHC* were very high. Higher fuel consumption was reported compared to conventional diesel combustion. Since the fuel is injected very early into an ambience with low temperature and density, preventing fuel impingement on liner walls or piston surfaces remains a challenging task. To reduce this over penetration and wall wetting, it is of great importance to optimize injector nozzle (narrow angle injectors, impinging nozzles), combustion chamber shape, injections strategies, and air management (boost pressure and swirl ratio). In order to improve combustion, an impinging spray nozzle injector was tested to generate wider dispersion angles and reduce penetration [33]. Consequently, fuel consumption was improved, soot and *UHC* emissions were considerably reduced. Various strategies can be applied to increase control robustness and load range of the HCCI combustion process.

Christiansen *et al.* [41] demonstrated first of high load HCCI results maintaining 14 bar IMPE by using supercharge technique (2 bar) and variable compression ratio. Their main conclusion was that the combustion phasing can be controlled by decreasing the compression ratio of the engine. Also Dec *et al.* [42] used the boosting technique and reported gross IMEP of 16 bar. They concluded that the key factor of good stability, high efficiency and low *NOx* was due to the retarded combustion phasing.

Foucher [43] exploit the effects of ozone on HCCI combustion. Addition of ozone at the intake of a HCCI improved the combustion because of the decomposition of ozone into

O-atoms. The results indicated that a controlled ozone concentration from 0 to 54 ppm improved the combustion and advanced the combustion phasing by 7 CAD. A further increase in ozone concentrations became less important due to only moderately effects on the combustion phasing.

2.2.2 Nissan Modulated Kinetics (MK)

Researchers at Nissan Motor Company [44, 45, 46] have carried out numerous studies on late direct-injection (near TDC) low temperature diesel combustion concepts, so that the combustion is more closely coupled to injection event. The basic thought is to inject the diesel fuel within a few crank angles and let the air and fuel mix during the ignition delay. Since the injection occurs near TDC, the combustion phasing can be controlled independently from the auto-ignition kinetics. This results in a combustion process that is dominated by a premixed burn condition.

To obtain LTC and the associated low emissions high injection pressure are to some extend required for rapid mixing, and various techniques must be applied to extend the ignition delay to allow more time for premixing. Kimura *et al.* [44] used a relatively common technique for extending the ignition delay, which is to retard injection (3 CAD aTDC) so that the jet mixing process occurs in the early part of the expansion stroke, slowing the auto-ignition. The addition of EGR to lengthen the ignition delay has the beneficial effect of lowering the flame temperature, which leads to low NO_X emissions. Rapid mixing was achieved by combining high swirl with toroidal combustion-bowl geometry. By avoiding the diffusion flame, the reported NO_X reduction was over 95% for MK operation compared to conventional diesel operation. Like other LTC concepts, issues to reach high load showed to be a limitation. In addition he also found out that techniques such as reduced CR and/or late IVC are often applied to increase the ignition delay.

Toyota Motor Company [24] reported a similar approach using excessive EGR levels (50%) to reduce the flame temperature to a level that results in no soot or NO_X formation. In this approach the EGR rate was used to reduce the flame temperature and the start of injection was advanced in high-EGR regimes. The amount of EGR required for low particulate formation decreased slightly as the EGR temperature was changed from 150°C to 100°C.

Miles *et al.* [47] performed an extensive study to examine the effects of increased EGR rates and retarding injection timing individually, coupled to images of natural luminosity from the combustion process. The optical diagnostics showed in-cylinder soot luminosity for EGR levels up to 60%. The findings indicate also that the MK combustion suffers from low combustion efficiency with high CO and UHC due to late combustion phasing.

2.2.3 UNIBUS

Another approach termed UNIBUS (Uniform bulky combustion system) was developed by Toyota Motor Corporation in order to reduce simultaneously NO_X and soot emissions [48]. This concept was utilized in the part-load regime and the engine is switching to diesel combustion at high loads. However, it was implemented in a production engine where the UNIBUS concept achieved by early injection strategy. To achieve LTC a split injections was applied. First fuel event was used early in the compression stroke, starting low temperature reactions, and the second one was injected near TDC to control the ignition of the resulting mixture.

2.2.4 RCCI

As mentioned above, the limitations of HCCI operation has further forced combustion research to promote new advanced combustion concepts. Therefore, recent investigations have focused on fuel reactivity control, which is often referred to reactivity controlled compression ignition (RCCI). This concept can be seen also as a dual-fuel CI, hence it relies on injection of two different fuels, one which is highly reactive and another which is less reactive. By varying the relative amount or timing of injection, both equivalence ratio and fuel reactivity stratification can be controlled.

It was found that combustion phasing could be controlled by the ratio of two fuels and consequently the engine operation range can be extended. For example, to use this strategy gasoline is injected trough PFI and a highly diluted mixture in the combustion chamber is created, which is ignited by a small amount of direct injected diesel fuel. The pressure rise rate (PPR) is lower and also the combustion rate for RCCI is much milder compared to HCCI operation, as can be seen in Figure 2.9.

The disadvantage of this concept is the requirement of using two separate injection systems. Thus, the complexity and cost of the engine are increasing considerably even when it provides a great flexibility of both combustion control and wider engine operation range compared to single fuelled HCCI engines. To find more detailed description of RCCI concept, the reader is referred to the works of [10, 50, 51, 52, 53, 54]

2.2.5 Partially Premixed Combustion

In recent years, a number of LTC concepts with various names and acronyms have been proposed in investigations and reported in the literature. Partially Premixed Combustion (PPC) is another type of advanced combustion concept which can simultaneously reduce the NO_X and the soot emissions. The distinction between HCCI and PPC is the degree

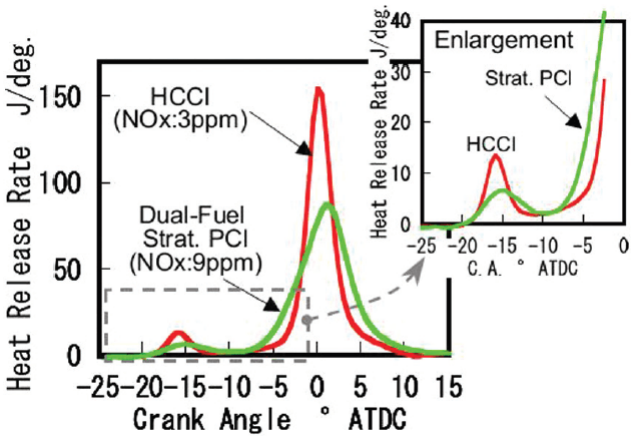

Figure 2.9: Comparison of RCCi vs. HCCI rate of heat release. Reproduced from [49].

of premixing of the fuel and oxygen. According to the LTC zone in Figure 2.3, many researches [55, 56, 57, 58] have ranged the LTC strategy broadly according to their fuel injection timing into two subcategories - early injection (injection well before TDC) and late injection (injection close to or even after TDC). A further attempt to categorize the LTC line was created by Dempsey *et al.* [59]. The authors divided the LTC concepts in three subcategories with the impact of fuel stratification on gasoline compression ignition: partial fuel stratification (PFS), moderate fuel stratification (MFS) and heavy fuel stratification (HFS). This fuel stratification depends among other things on both the duration of the final fuel injection and the auto-ignition delay of the mixture. In contrast to HCCI, the injection timing of fuel has a leading role for the PPC concept which further dictates the mixture strength and subsequent combustion phasing.

An essential feature of PPC is the ignition delay (ID) time, which is defined as the time poeriod between the end of injection (EOI) and start of combustion (SOC) measured in crank angle degrees. Therefore, it is of great importance to decouple the end of the injection from the start of combustion (positive ID) in order to achieve a moderate distribution of mixture strength (fuel stratification) just before the combustion takes place. However, a sufficient separation of injection and combustion allows a long period for the injected fuel to mix with the oxygen in order to avoid fuel rich zones and thereby soot formation. An excessive positive ignition delay can also lead to a large portion of premixed heat release, and thereby high pressure rise rates and higher noise levels, which can impose additional constraints on the required dilution level and injection timing. Conversely, if the ignition delay is negative (injection event not finished prior start of combustion), a diffusion flame will result and thereby the same dilemma will occur as in a diesel engine. Another mechanism to suppress smoke formation is achieved by low local combustion temperatures which

are below the needed temperature ($< 1800K$, illustrated in Figure 2.3) to form soot [24]. In low temperature regions the soot formation is suppressed, because pyrolysis reaction rates do not progress even rich combustion occurs.

Several research [60, 61, 62, 63] have carried out focusing on the potential of diesel partially premixed compression ignition (PPCI) concept for complying with stringent emissions limits in terms of NO_X and PM in both heavy and light duty engines. As it is expected other emissions including CO and UHC typically exceed regulated limits, so they still remain to be a common problem among these strategy. Hence practical diesel fuels are less residence to auto-ignition, common techniques like reduced CR, higher injection pressure, high EGR levels and early fuel injection timings were applied to extend the ID. In case of diesel fuel, shorter injection durations helps to achieve a positive ID, so that PPCI is typically employed for low load operations. The required long ID can also lead to excessive pressure rise rates and combustion noise at high fuelling rates, which limits also the PPCI to lower loads. Although, operating PPCI with diesel fuels has illustrated remarkable advantages in low emissions by utilizing a large amount of EGR to control the ID. Excessive EGR levels have shown a trade of, on one-hand they extend the ID and on other hand it is deteriorating the UHC and CO emissions and as a following consequence the fuel consumption and stability due to non-optimal heat release phasing.

Kook and Bae *et al.* [64] investigated the of charge dilution on low-temperature diesel combustion and emissions in a small bore single-cylinder diesel engine over a wide range of injection timing. Based on the findings in this work, charge dilution decreased the adiabatic flame temperature at a fixed start of injection. Furthermore, earlier injection events with high EGR level resulted in higher flame temperatures than seen with less dilution and later injection. They also reported CO emissions where increased due to incomplete premixing of a in-cylinder charge, as it is often referred in the the literature. But the CO emissions could be reduced, by injecting the fuel at earlier timings. Another work on PPCI was carried out by Kim and Ekoto *et al.* [61, 63], which have investigated the "smokeless" diesel or PPCI concept buy studying the effect of intake pressure on engine performance and emissions. They emphasised two injection strategies to achieve LTC: first, higher EGR with early fuel injection (SOI=-30 CA before TDC), second, moderate EGR rate with near TDC injection timing. Under the circumstances an increased intake pressure reduced the emissions of UHC and CO, with corresponding improvements in in fuel conversation efficiency and ISFC. Moreover, Soot emissions are reduced with increased intake pressure at high oxygen concentrations, but increased at low oxygen concentrations, while already low NO_X levels are achieved in both case.

In order to overcome the limitations of diesel-PPC, in 2006 Kalghatgi *et al.* [65] first proposed the direct injection of a fuel with high resistance to auto-ignition in CI engines. The experiments were conducted in a heavy duty engine and four different fuels including diesel and gasoline were investigated for the purpose of comparison. This pioneering re-

search work has successfully demonstrated the usage of gasoline to operate in PPC mode, by applying a single injection (25 CAD bTDC) and 10% EGR. The engine was operated at 1200 rpm by maintaining 14.86 bar gross IMEP, 46% indicated efficiency, 0.36 FSN and 1.21 g/kWh ISNOx. The main contribution to achieve this results was due to the significantly higher ignition delay of the gasoline fuel, which provides more time for fuel and air premixing prior auto-ignition compared to diesel fuels. Another remarkable outcome of this work is the crucial importance of fuel stratification to achieve auto-ignition in gasoline PPC. However, by injecting the same fuel quantity with early injection strategy was not capable, due to either misfire or excessive heat release. In contradiction, later fuel injection leads to heavy fuel stratification and as a consequence to a more stable combustion.

In his subsequent work [66] with the same engine, he further investigated the influence of an early pilot injection as a tool on reducing the rapid pressure rise rate, cyclic variation and as well as the emissions. The engine was operated with 1200 rpm, intake temperature of 40°C, intake pressure of 2 bar, 25% EGR and 23% of the total fuel amount was delivered in the pilot injection. By using a small fuel injection early in the compression stroke, the smoke level decreased compared to single injection, while the fuel consumption increased. As expected, the pilot fuel reduces considerable the spike of the heat release and allowed to retard the combustion phasing with low cyclic variations compared to single injection case. These advantages confirmed the potential of gasoline PPC operation to attain simultaneously low ISNOx (0.58g/kWh) and smoke emissions (0.07 FSN) with promising fuel consumption of 179 g/kWh at a mean load of 16 bar. At the same operating conditions, diesel fuel (Swedish MK1) had to have an IMEP below 6.5 bar to achieve similart low smoke values.

The comprehensive work achieved by Kalghatgi increased rapidly the interest in gasoline PPC in many research centres. Diverse institutes started to work on injection strategies which plays a crucial role in charge premixing and combustion phasing. In this sense, in 2010 Sellnau *et al.* from Delphi Powertrain enrolled the gasoline direct compression ignition (GDCI) engine concept for gasoline partially premixed compression ignition and has been under consideration and development for about five years. In [67] he reported important benefits in efficiency and emissions levels using dedicated engine hardware (piston and injector nozzle with narrow spray angle) properly optimized for PPC operation compared to using conventional hardware optimized for CDC. Moreover, he confirmed the potential of triple injection by using modelling methods for increasing thermal efficiency compared to a single injection strategy. This increase is thanks to reduced heat losses during the expansion stroke given by a more favourable fuel distribution during combustion which results in less contact between hot combustion gases and the chamber walls [68]. By adapting this injection strategy a lower injection pressure is needed compared to conventional diesel operations. For moderate loads of 6 bar IMEP the achieved results show a minimum fuel consumption of 181 g/kWh, while the obtained emissions were reported as

ISNOx of 0.7 g/kWh and smoke of 0.3 FSN. In the last development phase, the GDCI engine was operating from 1500-3000 rpm and measured BMEP of 20.3 bar using RON 91 gasoline fuel [69]. For these full load conditions, the experiments where performed with a air/fuel ratio close to stoichiometric conditions and cooled EGR was used with 40%, while the NO_X emissions where below 0.2 g/kWh and 0.2 FSN for smoke.

Most often, multiple injections are used with gasoline PPC to generate a suitable stratification of fuel/air in the cylinder at the time of ignition. Especially at high loads, double and triple injection can greatly help to decrease maximum PRR while still meeting the requirements acceptable efficiency and low NO_X and soot emissions. Foucher *et al.* [70, 71] used the double injection strategy to optimize the operation of gasoline-PPC mode in terms of heat release rate and pollutant emissions. The role of triple injection has been experimentally [72, 73, 74] and numerical studied [75, 76, 77] at medium and high loads. The common findings were, a significant amount of fuel can be injected fairly early (low density) in the compression stroke without causing any combustion because of the high resistance of the fuel to auto-ignition. The final fuel injection located close to TDC, was used to trigger the combustion by introducing the inhomogeneity in the mixture.

Following the initial attempts with gasoline PPC operation, Manente *et al.* [78] carried out comprehensive research work on different types of gasoline fuel for PPC operation. The fuel studies were conducted in a heavy duty single cylinder engine. The engine performance and emissions were investigated using an operable load range as a function of the fuel octane number for different types of gasoline-like fuels with RON spanning from 69-99. The engine load was swept from 5 - 25 bar with 50% EGR boosting to maintain λ=1.5. For the selected test conditions, 50% gross indicated efficiencies were reported with a peak of 57% at 8 bar IMEP. While the engine was able to operate in high loads with high RON fuels, however it was not possible to run low engine loads with high RON fuel due to misfire conditions.

Nonetheless, an important research effort has been made in the understanding of the PPC combustion strategy. Today, much of the research is focused on common investigations in terms of their respective pollutant emissions and efficiency level. As the literature review suggests, especially for PPC concept, there are some gaps to study in terms of in-cylinder combustion and flow characterizations. Therefore, the main motivation of this thesis is devoted to study how the combustion and bulk flow proceeds and how they are affected by employing different injection patterns. Furthermore, the study provides information in several areas as listed below:

- The combustion stratification is known to be a crucial feature for PPC concept. For this reason, a new approach was developed to determine the in-cylinder stratification level.

- The in-cylinder gas motion plays a significant role in mixture preparation and the ongoing combustion process. Therefore, the influence of injection strategies on the flow processes in the cylinder is examined by using the experimental velocity and turbulence fields.

- Cyclic variation is often represented by coefficient of variation (COV). In this work, cyclic variation was quantified by POD method. It is a technique that expresses the spatial structure of the flow in terms of the set of orthogonal basis functions (modes) that capture the highest fraction of the flow kinetic energy using the fewest modes.

- It is a common practice to estimate heat transfer coefficients by means of semi-empirical correlations. Nonetheless, heat transfer coefficient can be calculated with a different approach taking into account local velocities measured by PIV, as presented in this study.

- Combustion and emissions are characterized using gasoline-ethanol blend for PPC approach in a light-duty stock engine. An endoscope imaging system was used to acquire in-cylinder optical images of combustion events.

CHAPTER 3

EXPERIMENTAL EQUIPMENT AND OPTICAL DIAGNOSTIC METHODS

Most of the work underlying this thesis is based on optical diagnostics of in-cylinder physical processes. Several techniques are applied to characterize the behaviour of in-cylinder combustion, mixture formation and fluid motion in an optical engine. Transparent engines can be seen as a complementary research tools to constant volume or spray vessels. A spray vessel contains a controlled constant volume environment and is used to simulate the TDC conditions (pressure, temperature, density) for fundamental combustion research. While the conditions in optical engines are not as well-controlled as those in constant vessels, optical engines retain important features of stock engines that are not present in constant vessels (e.q piston bowl, swirl, bulk flow). In light duty engines for instance, optical access offers great opportunity to study the combustion process but also interactions and deflections of liquid spray with the bowl or with the charge motion.

3.1 Optical Research Engine

The experimental studies presented in this work are carried out in an optical engine based on a Volvo D5 series production engine, which is a five cylinder light duty compression ignition (CI) engine. For optical research purposes, the first cylinder of the base engine is converted to single cylinder operation and equipped with the Bowditch [79] piston extension. The remaining pistons are drilled trough in order to avoid compression nor expansion work. Additional mass is added to the motored pistons in form of tungsten alloy weights to balance the increased mass due to the piston extension. The Bowditch extension re-

quires that the cylinder head is separated from the cylinder block, where the extension is mounted on the original piston to provide a substantial optical access to the combustion chamber. A transparent piston made from fused silica is mounted on top of the elongated piston to enable optical accesses from below and from the side. In addition, a fully transparent liner (glass ring) is added to complete the assembly. Below the transparent piston, a 45° aluminium coated mirror is attached to the engine block to redirect the light from the combustion chamber to a camera next to the engine. An illustrative example of an optical engine with Bowditch design is given in Figure 3.1.a and the engine specifications are presented in Table 3.1.

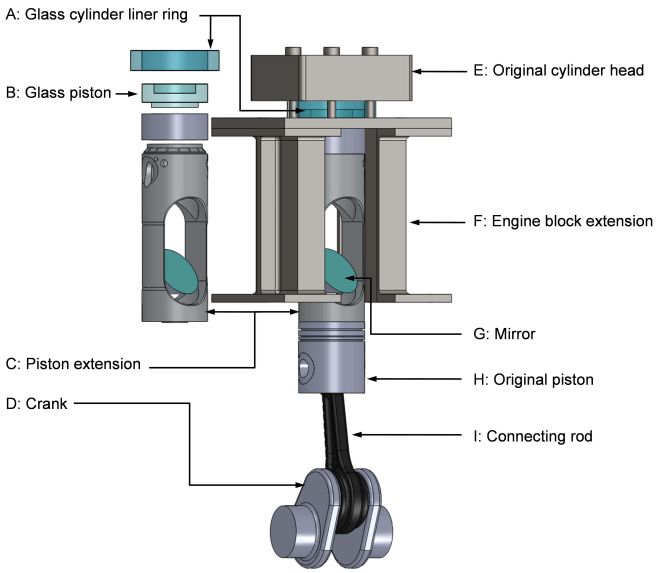

Figure 3.1: Schematic of Bowditch-type optical engine with details of the piston elongation assembly. Reproduced from [80].

Table 3.1: Geometrical engine properties and injectior specifications.

Engine specifications	
Displacement volume	0.48 L / cylinder
Stroke	93.2mm
Bore	81 mm
Connecting rod	147 mm
Compression ratio	11.5:1
Number of valves	4
Swirl	2.0 - 2.6
Injector specifications	
Fuel injection system	Bosch common rail system
Injector	5-hole/ solenoid actuated
Nozzle diameter	159 μm
Umbrella angle	140°
Hydraulic flow	360 cc/30sec at 100 bar

Despite the advantage of being able to studying more fundamental processes, there are some obvious limitations of optical engines due to the presence of transparent components. In most cases, synthetic fused silica pistons and quartz liners are used because they offer transparency in the ultraviolet region of the spectrum and are inexpensively compared to sapphire. Quartz parts lower the tolerable mechanical and thermal stress load of the overall structure, limiting the load range of optical engines. Due to having lower thermal heat conductivity than aluminium or steel, optical parts typically reach higher surface temperatures during operation. Therefore the heat transfer from hot gases to the liner wall is different compared to metal engines. To reduce the thermal load, optical engines are often operated in skip-fire mode. This means that the fuel is not injected during every cycle. In stead, a number of motored cycles follow on each fired cycle, limiting the wall temperature and preventing engine failures. Deformation of the piston extension during dynamic operation will affect the squish height between piston top land and the fire deck [?]. The effective compression ratio is thereby lower for optical engines. Finally, a significant feature of the Bowditch design is the difference in piston rings compared to a metal engine. Metal piston rings that make up to seal between pistons and cylinder wall are usually lubricated by the engine oil. For optical configuration this is not desirable as the lubricant could interfere with the optical measurements and lead to bias. For this reason, optical engines are fitted with dry piston rings. The piston rings used in these work was custom made using a lathe out of Rulon, a material with very low coefficient of friction. A drawback of this piston rings are that they cannot be operated at elevated temperatures, which can be overcome by using skip-fire as mentioned before. The piston rings are also placed lower on the piston compared to a metal engine, to prevent the rings from passing across the joint between the optical and metal parts. This lower position increases the clearance volume and thus the effective compression ratio decreases.

Another approach of optical access without heavy modifications of the base engine are imaging techniques with endoscopic access to the combustion chamber, which was used in Paper VII. The main advantage of using an endoscope are the small dimensions of the optics involved into a constrictive space in which conventional optics do not have sufficient space. The small size of the endoscope enables to keep the original geometry of the engine to be unchanged. This allows to perform the engine under as realistic conditions as possible.

All the acquired 2D image data presented in Paper VII used an endoscope with 70 degree window. Although, the endoscope accesses the combustion chamber via steel sleeve with the pressure-resistant window that protects the endoscope. Such combustion chamber windows are designed to withstand the pressure and temperature conditions of usual engine operating modes. With adequate design and material selection, window applications include full load operation in both diesel and gasoline engines. The endoscopic optics consists of many parts: endoscope, protection glass, steel sleeve and the camera. The setup of the endoscope system and the endoscope assembly are given in Figure 3.2.

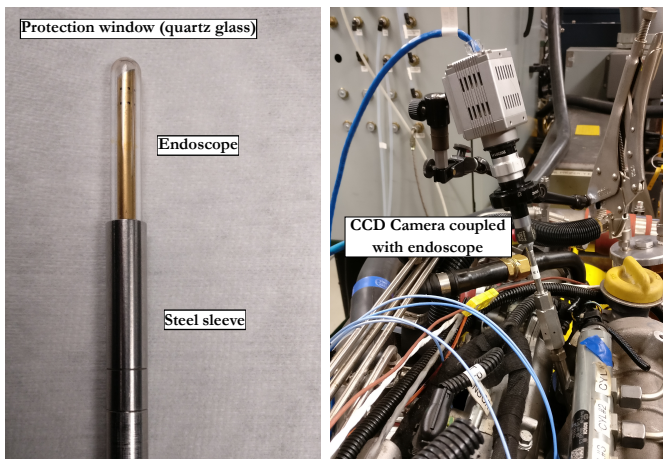

Figure 3.2: Left: Endoscope probe protected by a sealed sapphire window. Right:Endoscope fitted in the cylinder head of a diesel engine.

3.2 Heat Release Analysis

Although this thesis focuses on optical diagnostics of the combustion process and fluid motion, the rate of heat release provides essential information about the combustion process during the cycle and how it correlates with the optical experiments. To perform a heat release crank angle resolved analysis, pressure sampling is necessary. The cylinder head is fitted with a piezoelectric sensor to detect the in-cylinder pressure trace. The measured

pressure data are evaluated by using a single zone model. This model assumes that the combustion chamber space is an ideal mixed volume, where pressure and temperature are uniform, and does not distinguish between burned and unburned gases. Figure 3.3 shows a schematic of the combustion chamber with thermodynamic definitions.

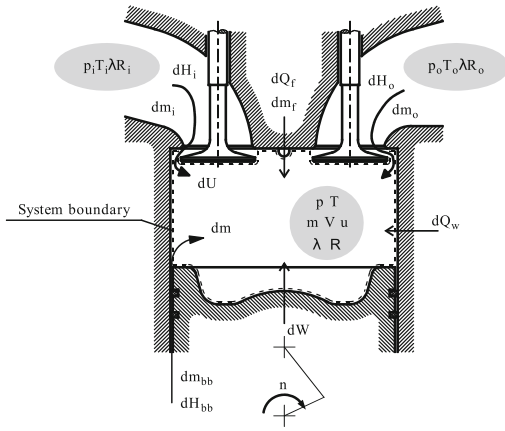

Figure 3.3: Single-zone model for heat release analysis. Reproduced from [81].

The following approach is a description of the Heywoods [6] heat release theory. The heat release analysis is based on the first law of thermodynamics, given in equation 3.1. The energy balance is defined by the internal energy of the charge, the work performed by the system on the piston, the heat transfer to the cylinder walls, and energy loss by blow-by.

$$dQ = dU + dW + dQ_{\mathrm{HT}} + dQ_{\mathrm{Crevice}} \tag{3.1}$$

Using the ideal gas law and the mass conversation law, the heat release per crank angle can be described as:

$$\frac{dQ}{\theta} = \frac{\gamma}{\gamma - 1} p \frac{dV}{d\theta} + \frac{1}{\gamma - 1} V \frac{dp}{d\theta} + \frac{dQ_{HT}}{d\theta} + \frac{dQ_{Crevice}}{d\theta} \tag{3.2}$$

Where pressure p is measured, volume V is calculated from the engine geometry and γ is the the specific heat ratio C_p/C_v.

The heat exchange between the in-cylinder charge and combustion chamber surface (cylinder wall, cylinder head and piston) is described by convection, Eq. 3.3. To estimate heat transfer coefficient h_c, an empirical model introduced by Woschni *et al.* [82] is used, Eq. 3.4. The Woschni model is based on the Nusselt-Reynolds relationship, where C is an engine specific constant, B is the cylinder bore in m, p is pressure in kPa, T is the in-cylinder charge temperature in K and w is the characteristic gas velocity in m/s. Woschni's approach was to relate the gas velocity to the mean piston speed. The characteristic velocity

is described in Eq. 3.5. Here, V_d represents the displacement: V_{ref}, p_{ref}, T_{ref} are a reference volume, pressure and temperature at IVC, respectively. C_1 and C_2 are coefficients used to the tune heat transfer model for the specific engine. Finally, p is the actual pressure and p_{mot} is the motored pressure

$$\frac{dQ_{HT}}{dt} = h_c A_{wall}(T_{gas} - T_{wall}) \tag{3.3}$$

$$h_c = CB^{-0.2} p^{0.8} T^{-0.55} w^{0.8} \tag{3.4}$$

$$w = C_1 S_p + C_2 \frac{V_d}{V_{ref}} \frac{p - p_{mot}}{p_{ref}} T_{ref} \tag{3.5}$$

3.3 Chemiluminescence imaging

Traditionally, combustion visualization using high speed camera is commonly used within the field of optical combustion diagnostics. The combustion process is characterized by many chemical reactions that occur in the flame front and create a region of high local heat release. Thus, a great deal of the combustion research focuses on visualization of the combustion progress trough the engine cycle. One important intermediate species in the oxidation of hydrocarbon fuels is the hydroxyl-radical (OH*). For the most part, OH radical remain in the ground state, whereas in high temperature regions it appears in excited state [83]. To distinguish OH in excited state from ground state, it is usually marked by a star, OH*. Followed by relaxation to ground state OH* emits signal trough spontaneous photon emission, the appearance of this emission is referred to OH* chemiluminescence. Therefore, OH* is a commonly used as a marker of the high temperature reactions.

In the present study, OH* chemiluminescence imaging is used because the method offers possibilities to draw qualitative conclusions such as spatial auto-ignition location and combustion propagation trough the engine cycle. Crank-angle resolved combustion luminosity was recorded with an Hamamatsu image intensifier unit, a 105mm UV-Nikkor lens and an OH* interference filter to capture the chemiluminescence of OH* radicals. A band pass filter centred at 310 nm was used for the subtraction of OH* chemiluminescence from the background signal. An illustrative schematic of the experimental setup is presented in Figure 3.4.

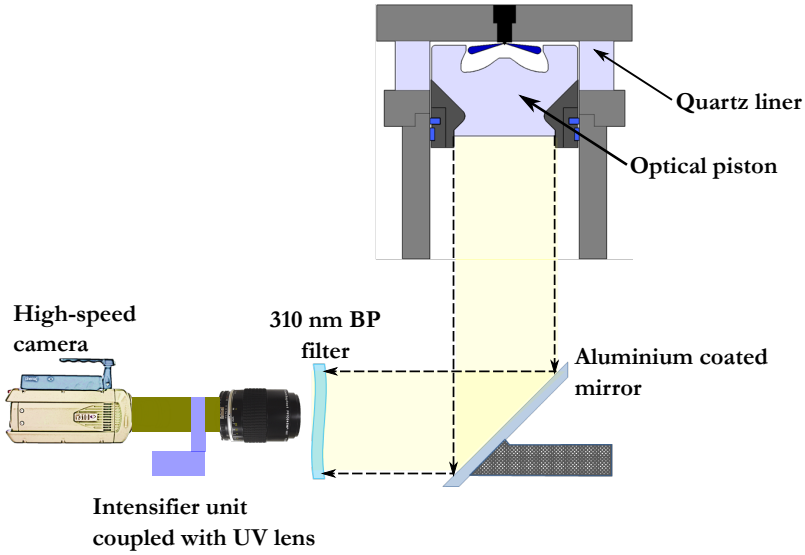

Figure 3.4: Schematic of OH* chemiluminescence method.

3.4 Experimental flow field analysis

3.4.1 Particle Image Velocimetry PIV

The basic principle behind measuring fluid velocities with PIV can be described briefly:

1. Use seeding particles that can follow the fluid
2. Record two images of the seeded fluid
3. Calculate the velocity vector from the displacement of the particles between the two images in a known time interval

The PIV method requires a synchronization with the engine speed and a high-speed camera. This is achieved by a so-called synchronization unit, which helps to trigger the two laser shots according to the crank angle position and recording of the images. The layout of the PIV setup is shown in Figure 3.5. The PIV technique implies a thin slice of the investigated flow field to be illuminated by a laser sheet. Particles within the sheet scatter the light, which is detected by a camera placed perpendicular to the laser sheet. The flow field is usually illuminated by a double-pulsed laser with a known time separation, Δt. The first pulse of the laser records the initial position of the particles onto the first frame of the

camera. Accordingly, the second frame of the camera is exposed by the the scattered light from the second laser pulse with a time delay Δt. The time separation between the two light pulses are to be sufficiently long to be able to determine the displacement.

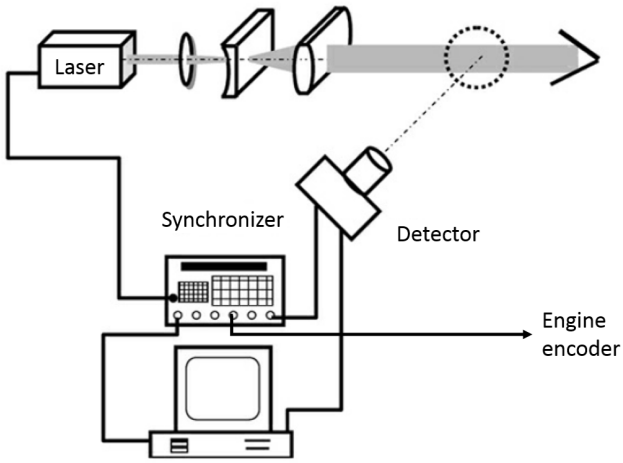

Figure 3.5: Schematic of a typical PIV setup. Reproduced from [84].

Consequently two images are saved, the first showing the initial position of the particles and the second their final positions due to the movements of the flow. Those two frames are subsequently divided into a number of regions called interrogation areas (IA). An arbitrary IA in the first frame is compared with the corresponding IA in the second frame. The displacement and the direction of this movement are evaluated by a cross-correlation algorithm. The cross-correlation method [85, 86] is not applied to the entire frame, but to subdivided interrogation windows. The evaluation of cross-correlation from a single IA is used to determine the position of the displacement peak, which corresponds to the velocity vector. A typical result of the cross-correlation method is illustrated in Figure 3.9. The result from one IA contains the terms R_F and R_C, which contributes to the fluctuating background noise and (R_D) represent correlation peak in the correlation plane.

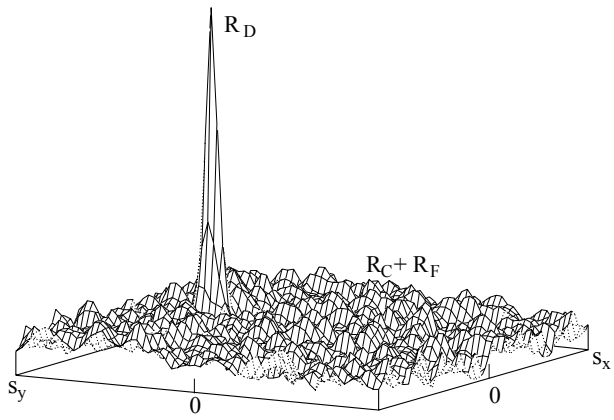

Figure 3.6: Cross-correlation result of two images showing the displacement peak R_D, the fluctuating component R_F and the convolution of the mean intensities R_C. Reproduced from [85].

Calculation of the cross-correlation, between two interrogation windows results in a single velocity vector showing the direction of the fluid motion. The fluid flow is obtained by processing all the interrogation areas. In order to significantly increase the accuracy of the velocity vector calculation, an adaptive PIV method in the software were used which could iteratively adjust IA size, shape and orientation according to the result of iterations. The interrogation area (IA) was chosen to be 64 x 64 pixels as an initial value which is iterated down to 12 x 12 pixels.

Application of PIV in reacting flows is associated with various additional challenges not found in typical aerodynamic applications. Most importantly the seed material must withstand high temperatures without chemically interacting with the in-cylinder flow under experimentally investigation. Metal oxide powders such as silica, alumina or titanium oxide (TiO_2) are generally well suited for this purpose due to their high melting point and availability [85]. In this study, TiO_2 is introduced into the intake stream by using fluidized cylindrical container fed by a swirl airflow of around 20 liters/min. Seed particles have an average particle diameter between $3\mu m$ and a density of 4260 kg/m3. Assuming Stokes drag, the particle time constant (τs)-representing the response time to changes in the flow-is roughly $40\mu s$ under TDC-like thermodynamic conditions.

Vertical imaging trough an optical piston bowl causes a significant distortion that had to be corrected to obtain valid velocity vector maps. An image of dot target with $1mm$ spacing between the dots was placed in the field of view of the camera. This correction was used for the results in Paper II - Paper VI. The distortion correction routine was performed using a function build in Matlab (R2013a). Figure 3.7 shows an example of the distorted target image and and its correction. The same procedure was separately applied for the squish

region, even the distortion effect was less compared to the bowl region. After correction of the distortion for bowl and squish region, the full image is obtained by merging these two regions together.

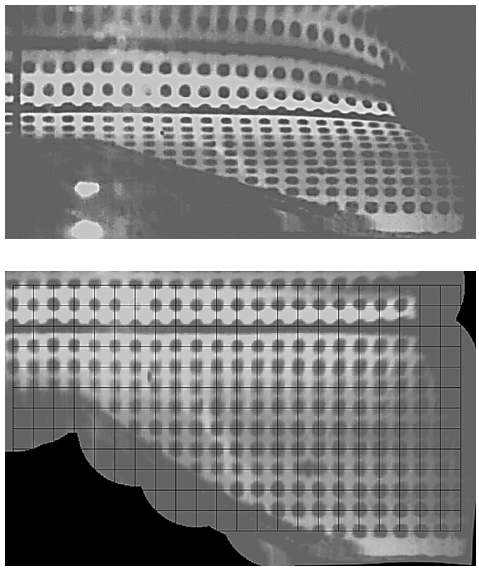

Figure 3.7: Top: Distorted target image of the half of bowl-in-piston design.
Bottom: Corrected target image of the half of bowl-in-piston design

3.4.2 Velocity and Turbulence

The nature of in-cylinder flow is a complex phenomenon, widely characterized by an unsteady turbulent flow. The character of turbulence can thereby be defined by fluctuations about an average velocity, as depicted in Figure 3.8. The following description of velocity and turbulence theory is based on [6, 14].

The instantaneous velocity $U(\theta, i)$ consists of the phase average (ensemble average) mean velocity, $\bar{U}_{\mathrm{EA}}(\theta)$, and the turbulent fluctuation about it, $u'(\theta, i)$, where θ is the crank angle position, i is the engine cycle index and N is the total number of cycles:

$$U(\theta, i) = \bar{U}_{\mathrm{EA}}(\theta) + u'(\theta, i)_{\mathrm{EA}}, \tag{3.6}$$

where $\bar{U}_{\mathrm{EA}}$ is given by:

$$\bar{U}(\theta)_{\mathrm{EA}} = \frac{1}{N}\sum_{i=1}^{N} U(\theta, i). \tag{3.7}$$

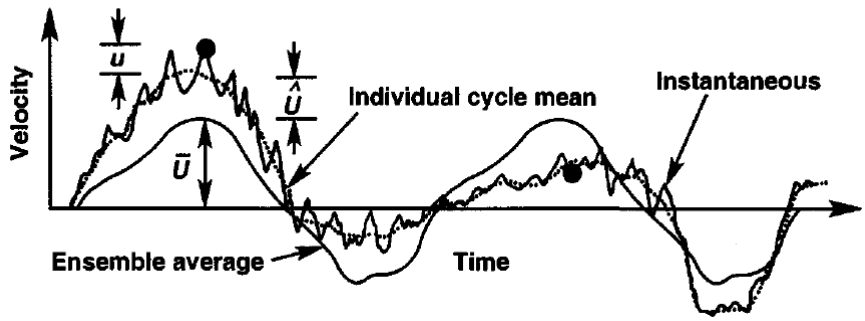

Figure 3.8: Crank-angle resolved velocity variation during two representative engine cycles for instantaneous, phase averaged and individual cycle mean velocity. Reproduced from. Reproduced from [14].

An important meaning of Equation 3.7 is that $\bar{U}_{\mathrm{EA}}(\theta)$ is a function of crank angle alone, which implies that the mean flow at a particular position has no cycle to cycle variation. In order to consider the cycle to cycle variation, the in-cycle or individual cycle mean velocity $\bar{U}(\theta, i)$ has to be calculated. The approach used in this work is the moving window average [87] in the crank angle domain. This method implies a correct selection for a crank angle window on the basis of being larger than the small scale turbulence, but smaller than the characteristic period of the piston motion. A window size of 10 crank angles where applied to the individual velocity data. Firstly, the mean velocity is taken as the mean within a crank angle window $\Delta\theta$:

$$\bar{U}(\theta, i) = \frac{1}{N} \sum_{\alpha=\theta-\frac{\Delta\theta}{2}}^{\alpha=\theta-\frac{\Delta\theta}{2}} U(\alpha, i) \tag{3.8}$$

where $\Delta\theta$ is the interval within which the samples are averaged to get the mean velocity. The cut-off frequency at which the flow is separated to slowly varying mean velocity variations and faster high-frequency turbulence requires some comments. If a wide $\Delta\theta$ is selected in the calculation of mean velocity the cut-off frequency will be lower and hence less information is contained in the mean velocity variation from cycle to cycle.

The turbulence is extracted by noting how much the individual velocity registrations differ from the low pass filtered mean velocity at the same crank angle position.

$$u'(\theta,i) = \sqrt{\frac{1}{N}\sum_{\alpha=\theta-\frac{\Delta\theta}{2}}^{\alpha=\theta-\frac{\Delta\theta}{2}} \left(U(\alpha,i) - \bar{U}(\alpha,i)\right)^2} \tag{3.9}$$

The mean value of cycle resolved velocity at each CAD for all the cycles could be expressed as:

$$\bar{U}(\theta)_{\text{cyle}} = \frac{1}{N}\sum_{i=1}^{N} \bar{U}(\theta,i) \tag{3.10}$$

Furthermore, the mean value of turbulence for a specific CAD for all cycles is given by:

$$u'(\theta)_{\text{cyle}} = \frac{1}{N}\sum_{i=1}^{N} u'(\theta,i) \tag{3.11}$$

The turbulent kinetic energy (TKE) within an interrogation area (IA) could be expressed by:

$$TKE_{x,y} = \frac{1}{2}[(u'_{x,y})^2 + (u'_{x,y})^2] \tag{3.12}$$

In Equation 3.12 u and v represent the turbulence in the horizontal and vertical directions, respectively, where x and y indicate the position of different interrogation areas in the piston bowl.

3.4.3 Turbulent flow field decomposition - POD

A promising approach for studying turbulent engine flows is the phase invariant proper orthogonal decomposition (POD) technique. This technique provides a classification method based on an energy criterion by which the mean flow is seen as a superposition of coherent structures. From their temporal coefficients it is possible to characterize its dynamical behaviour.

POD, is closely related to Principal Component Analysis, PCA, from linear algebra and was first introduced in the context of Fluid Mechanics by Lumley *et al.* [88]. This implementation of POD applies the so-called Snapshot POD proposed by Sirovich *et al.* [89]. Each instantaneous PIV measurement is considered as a snapshot of the flow. An analysis is then performed on a series of snapshots acquired in the same position and under identical experimental conditions. The first step is to calculate the mean velocity field from all the snapshots. The mean velocity field is considered the zero'th mode of the POD. Subtracting

the mean from all snapshots, the rest of the analysis operates on the fluctuating parts of the velocity components (u_{mn}, v_{mn}) where u and v denote the fluctuating part of each velocity component. Index m runs through the M positions (and components) of velocity vectors in each snapshot and index n runs through the N snapshots so $u_{mn} = u(x_m, y_m, t_n)$. All fluctuating velocity components from the N snapshots are arranged in a matrix U such that each column contain all data from a specific snapshot:

$$\mathbf{U} = [U^1 U^2 ... U^N] = \begin{pmatrix} u_1^1 & u_1^2 & \dots & u_1^N \\ \vdots & \vdots & & \vdots \\ u_m^1 & u_m^2 & \dots & u_m^N \\ v_1^1 & v_1^2 & \dots & v_1^N \\ \vdots & \vdots & & \vdots \\ v_m^1 & v_m^2 & \dots & v_m^N \end{pmatrix}$$

Figure 3.9: Data matrix, consisting of the set of all data vectors at a specific point in time[DS]

Using the velocity matrix U the correlation matrix, or auto-covariance matrix, is defined as:

$$R = \mathbf{U}^T \mathbf{U} \tag{3.13}$$

Furthermore, the eigenvalue problem of auto-covariance matrix R can be solved as:

$$RA = \lambda A \tag{3.14}$$

The eigenvectors (A) are sorted in the same order as the eigenvalues and stored as a matrix used to define the POD mode matrix (U) which is normalized:

$$\theta = \frac{A\mathbf{U}}{\|A\mathbf{U}\|} \tag{3.15}$$

The POD coefficients (a_i) for a specific snapshot are determined by projecting the velocity field of the snapshot onto the POD modes:

$$a_i^n = \phi^i \mathbf{U}^n \tag{3.16}$$

Using the POD coefficients and the POD modes, a snapshot (n) can be reconstructed using:

$$U_r^n = \sum_{i=1}^{i_{max}} a_i^n \phi^i \tag{3.17}$$

When all POD mode contributions are included (imax = N), the snapshot is fully reconstructed.

CHAPTER 4

RESULTS

The work in this thesis is primarily focused on addressing the in-cylinder bulk motion under gasoline-PPC conditions. The fuel used for the experiments was prime reference fuel PRF 70, with an octane number of 70. Principally the impact of different injection timings and split injections on the flow pattern, turbulent kinetic energy and cyclic variations have been investigated.

Apart form the PIV results, both chemiluminescence and endoscopic imaging results are discussed as well in chapter number. The interest lies in maintaining the stratification level which is crucial for gasoline PPC (as described in section 2.2.5).

4.1 The role of multiple injection strategy under PPC condition

This study is described in Paper I and is used to determine the combustion stratification by employing multiple injection strategies. Fuel and thermal stratification are potential strategies for reducing the maximum pressure rise rate in gasoline fueled CI engines [90, 91, 92, 93]. It has been observed that small modifications of the injection events can alter the charge stratification and consequently the entire combustion process significantly. It is thereby important to achieve the right mixture conditions (for stratification level) to prevent overmixing of fuel and air, which leads to HCCI like combustion. On the other hand, it is crucial to not trap into the NO_x and soot formation islands by late fuel injection timing, which reduces the mixing time is reduced. Advancing fuel injection enough to achieve a moderate mixing of the charge will lead to partial premixing i.e. PPC [13]. As

explained in Chapter 2.2.5, it is essential for PPC to achieve positive ID time in order to permit sufficient mixing for soot reduction.

Figure 4.1 shows the characteristics of PPC process, where the upper figure 4.1.a illustrates the heat release history and images below (4.1.b) show the hydroxyl radicals (OH*) throughout the combustion process for various injection cases. Negative valve overlap (NVO) was applied for controlling of combustion stability. The NVO strategy incorporates early exhaust valve closing (EVC) and late intake valve opening (IVO) in order to retain large quantities of residuals. NVO thereby provides, in an efficient manner, the thermal stratification and dilution advantages of the charge by retaining residuals.

Most often, multiple injections are used with PPC to generate a suitable stratification of fuel/air in the cylinder at the time of ignition and in order to shape the heat release rate [72, 73, 74, 75]. The first observation from Figure 4.1.a shows the similar behaviour of the heat release shape for single and double injection. The single injection case, an injection timing of -6 CAD aTDC was used and a dwell time of 515µs. For the double injection case, the injection timings were -60 and -6 CAD aTDC, and the dwell times 450µs and 380µs, respectively. As a consequence of the early fuel injection in the double injection case, the combustion peak and therefore the combustion phasing is retarded few crank angle than for the single injection. The fuel from the first injection is used to stratify the low density charge without promoting combustion. During this phase (long ID), the injected fuel has sufficient time to mix with the surrounding air. As the density of the premixed charge increases, the fuel from second injection is employed to trigger the combustion.

The triple injection case gives another clear trend, compared to the other injection strategies. It can be seen from 4.1.a that maximum heat release rate can indeed be reduced by using multiple injections but probably at the cost of higher *UHC* and *CO* emissions [72]. The pressure and heat release rate can be changed by redistributing the fuel injection into three pulses with the first SOI at -50,the second SOI at -28, and the third SOI at 5 CAD aTDC. The triple injection strategy in which the first injection was set early enough for the fuel to be nearly homogeneous and still too lean to auto-ignite, and thus did not form any combustion products. The second injection was late enough to retain some local richness and mixture stratification to provide sufficient fuel and air premixing to not form significant amounts of *PM* or NO_x during the combustion process. In general, the ignition timing could be controlled by the timing and quantity of the fuel in the second injection. Finally, the third injection was performed near TDC to trigger the combustion and add load without increasing combustion noise.

To understand the observed differences in the RoHR curves for the different injection timings, high-speed camera sequences showing OH* chemiluminescence were recorded. Since the hydroxyl radical, OH*, is formed during the high temperature reactions in combustion and is a highly reactive species, visualization of OH* formation during the combustion

process is a widely used measurement method [51, 55]. The image sequences for the three

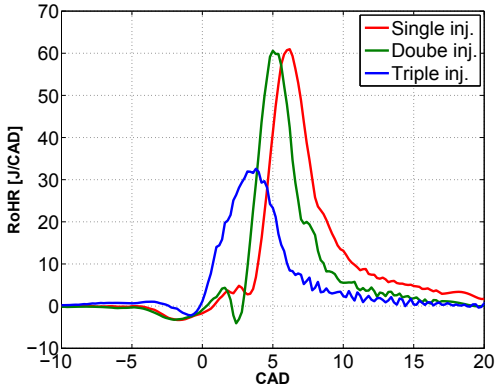

(a) Heat release rate for single, double and triple injection events.

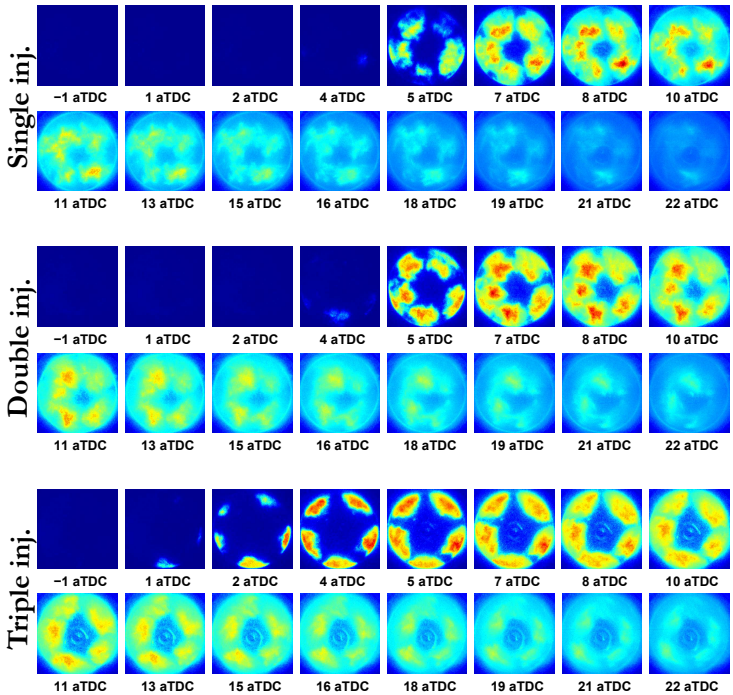

(b) Luminosity images of the PPC combustion sequence for single, double and triple injection.

Figure 4.1: Rate of heat release and PPC combustion imaging for multiple injection strategies.

selected injection timings are shown in Figure 4.1.b. The camera settings were held fixed for all operating conditions. The images are acquired with the high-speed camera viewing upward through the optical piston window and the imaging setup is discussed in section 3.3. The image sequences presented here are from a representative single cycle that has the heat release most similar to the ensemble averaged RoHR curve.

The images for single and double injection show similarities in consistency with their RoHR shapes. In both cases, the first signal from the high temperature reaction are captured at 4 CAD aTDC. The appearance of the chemiluminescence at this timing for the double injection case shows several ignition zones in the lower part of the piston bowl. It can be assumed that premixed charge reached the "preferred" equivalence ratio to initiate locally auto-ignition. After auto-ignition at 4 CAD aTDC, the premixed charge ignites rapidly. Thereafter, between 5 CAD and 15 CAD aTDC the fuel is consumed and preferential reaction zone growth direction are controlled by gradients in the fuel reactivity. At this point, it should be stated that at 5 CAD aTDC, five individual combustion clouds are observed, corresponding to the same number of injector nozzle holes. These chemiluminescence images also indicate the bulk movement reaction zone, namely away from the piston bowl edge inward toward the center of the combustion chamber.

As discussed above in connection with the RoHR analysis, the triple injection case gives an early combustion of the premixed charge. By 1 CAD aTDC, small auto-ignition pocket is initially observed in one location. Just 1 CAD after this, OH-radicals appear in small pockets in several locations inside the edge of the piston bowl rim, representative of the 5-hole nozzle. These ignition zones grow during several crank angle degrees while more ignition pockets continue to appear. The separate ignition pockets then merge into larger, more coherent reaction zones. Compared to the single and double injection cases, the combustion zone is most consistent at the outer region of the combustion chamber.

4.1.1 Combustion Stratification

The objective of this study was to determine the stratification level and demonstrate a methodology to compare the injection cases and gain a preliminary understanding of the PPC combustion evolution. The preliminary high-speed OH* chemiluminescence imaging provides an excellent overview of the combustion process and allows the progression of the reaction zone to be observed in the a single-cycle. Chemiluminescence imaging is a simpler technique which uses chemical excitation instead of laser light. The camera records the light emitted from the chemically excited OH, denoted OH*, see Chapter 3.3.

Figure 4.2.a shows a image divided in 8 annular bands with a width of 15 pixels. Because the curved combustion chamber walls induce significant optical distortion, the images of the combustion chamber were first divided in eight annular narrow bands to analyze the

degree of stratification in each band. To determine the angular stratification, the intensity is radially averaged and plotted as a function of polar angle Θ. Figure 4.2.a shows a typical behaviour of PPC combustion by applying this method to each frame (CAD) of an OH*-chemiluminescence movie. Based on that, the range of Θ can be divided to 5 equal segments, representative of 5 combustion zones, presented in Figure 4.2.b.

From Figure 4.2.b the difference of the intensity ($\Delta I = I_{max} - I_{max}$) for each spray was calculated together with the mean intensity of each band for each crank angle. The degree of stratification was determined as a ratio between the differences of the intensity over the mean.

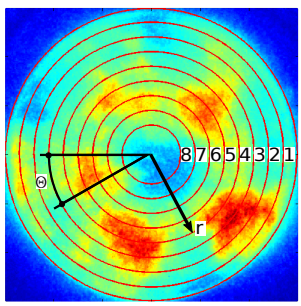

(a) The combustion chamber is divided in 8 annular bands; theta illustrates the rotational angle and r indicates cylinder radius in polar coordinate.

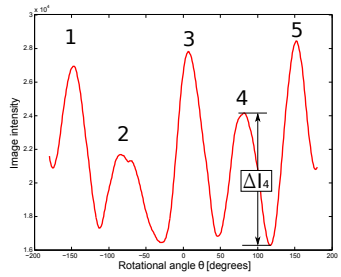

(b) Image intensity as a function of the angular angle theta in cartesian coordinate.

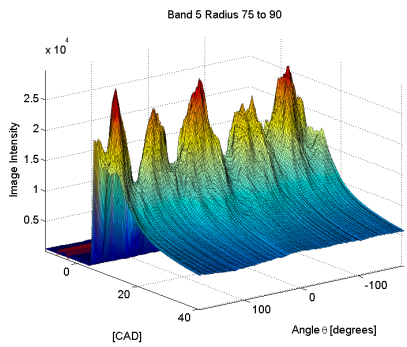

(c) Combustion intensity as a function of theta for a sequence of CADs (back view).

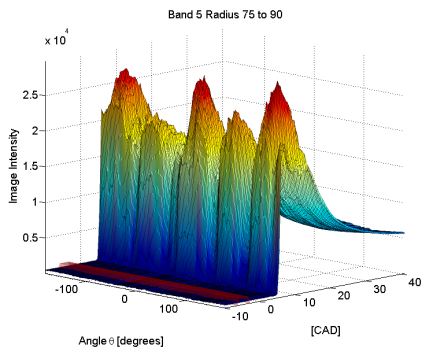

(d) Combustion intensity as a function of theta for a sequence of CADs (front view).

Figure 4.2: 2D and 3D intensity plots for a given CAD.

Figures 4.1.c and 4.1.d depict the image intensity as a function of the rotational angle and presents two different views of five individual spray areas with different maximum

intensity peaks. The red semi-transparent bar represents the single or last fuel injection pulse. An important observation is that the five sprays have different peak intensity, which is an indication of stratified combustion. The spray peaks have different intensities strength, because of different local equivalence ratios. If the local equivalence ratio matches the global equivalence ratio, then the combustion will be HCCI type and less fluctuation of the corresponding peaks will be obtained. Furthermore, it is interesting to note that the steep increase in OH*-signal is associated with the high temperature reactions during the combustion and is decreasing in accordance with the RoHR when the combustion decays.

Finally, Figure 4.3 shows the stratification level for all three injection events. The stratifications levels are showing a great consistency with the shape of the RoHR curves. It is clearly shown that for the triple injection case, the stratification level decreased compared to the single and double injection cases. The relatively long ignition delay and high volatility of gasoline, combined with an advanced injection system and variable valve actuation, provides controlled mixture stratification for low combustion noise. Redistribution of the fuel injection pulses leads into higher homogeneity of the premixed charge and is often used to achieve high load operations [75].

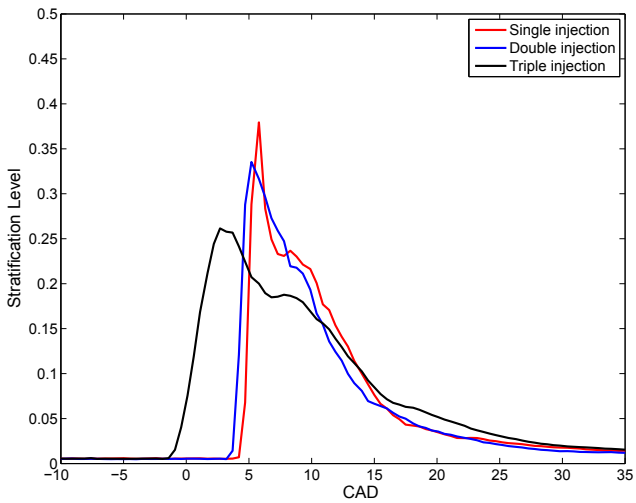

Figure 4.3: Degree of Stratification for single, double and triple injection as a function of CAD.

4.2 In-Cylinder flow characterization under PPC conditions

Flow field measurements were carried out in a light duty optical engine to characterize the effects of different injections strategies (single, double and triple injections) on the cycle resolved mean flow, turbulent kinetic energy (spatial and temporal) and cyclic variations.

The results in section 4.2.1 corresponds to experimental data presented in Paper IV, and discuss the vector fields in the clearance volume and bowl region. This study describes in detail the formation of fluid motion during the compression and expansion phases. As pointed out by many researchers, the in-cylinder process in automotive engines have a far more important role than filling and emptying the combustion chamber [14, 6]. Flow structures are essential to the fuel-air mixing process, trough both large-scale bulk transport by the mean flow and the small-scale mixing by the turbulent eddies. The main aspect of the present section is primarily focused on the influence of the fuel injection event on formation of large-scale bulk flow structures, and on the turbulence that these structures generate.

4.2.1 Effects of split injections

In this study, combustion phasing (CA50) was kept constant at around 8 CAD aTDC. Multiple injections were used to achieve less fuel stratification due to more premixing of fuel. As presented in Paper I, double and triple injection cases demonstrate less fuel stratification compared to single injection. The premixing is promoted using PRF 70 as fuel, and fuel injection early in the compression stroke to increase the ignition delay. It can be seen from Figure 4.4 that the maximum heat release rate can indeed be reduced by using multiple injections. As seen from the single injection case (SOI = -17 CAD aTDC), the fuel rapidly mixes with the ambient oxygen and due to the high octane number (RON 70), the ignition delay give intent to a sharp heat release, and consequently a high pressure rise rate. To overcome these issues, multiple injection strategies with early injection pulses are employed to promote different levels of fuel stratifications. The associated in-cylinder flow pattern for single, double and triple injections under combustion conditions will be presented in the following section.

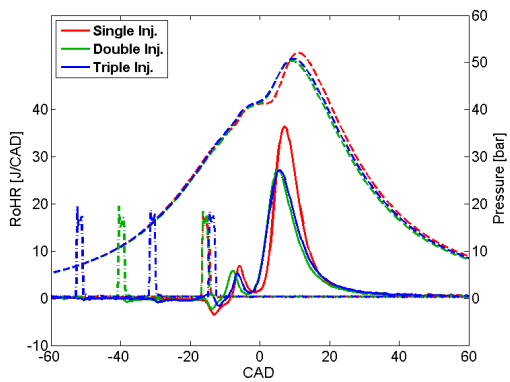

Figure 4.4: Pressure an heat release rates at constant combustion phasing (CA50 = 8 CAD aTDC).

Compression phase

The flow in the cylinder is divided into several distinct phases for each split injection from -45 to 35 CAD aTDC. Figure 4.5 shows the mean flow fields during the compression stroke from -45 to -25 CAD aTDC for three cases (single, double, and triple injection respectively). At -45 CAD aTDC the ensemble average flow fields for the single and double injection cases are showing similar in-cylinder behaviour. During this position, the flow fields are directed upwards according to the piston motion and the flow structure is mainly governed by the air flow into the cylinder trough the inlet ports and valves. As compared with triple injection case, the flow pattern at this piston position differs greatly. For the triple injection case the engine cycle starts with a fuel injection at -55 CAD aTDC during the compression stroke, which leads to a change in the squish flow pattern. Because of the fuels auto-ignition resistance, the injected quantity does not react and is mainly timed to mix sufficiently with the intake air. However, due to low gas density and fuel volatility, the injected fuel also impingements on the cylinder liner and this wall wetting has an important effect on the resulting *UHC* emissions [94]. Similarities were obtained for the double injection case, while the pre-injection event at -40 CAD aTDC leads to a change of the flow pattern due to the injection process. It can be seen that high pressure fuel injection has a great influence on the flow pattern, inducing high radial momentum into the system. The effect of the spray on the bulk flow structures will be discussed later.

When the squish volume is further compressed from -40 to -25 CAD aTDC, the flow above the piston squish area splits into two parts. During the vertical movement of the piston, the fluid elements were displaced inward toward the cylinder centerline. A clear example for the single injection case can be seen in Figure 4.5. In addition, the squish flow follows the horizontal track caused by the deflection of the strong bulk motion and swirl flow. As the piston-bowl enters the field of view at -30 CAD aTDC , it should be noted that the squish flow in the corner is redirected towards cylinder centerline (for the triple injection case). This flow manipulation is accomplished trough external stimulus, such as the second fuel injection process. Thereby, the generation of new structures can efficiently transport fuel or combustion products out of the squish region towards central part of the combustion chamber.

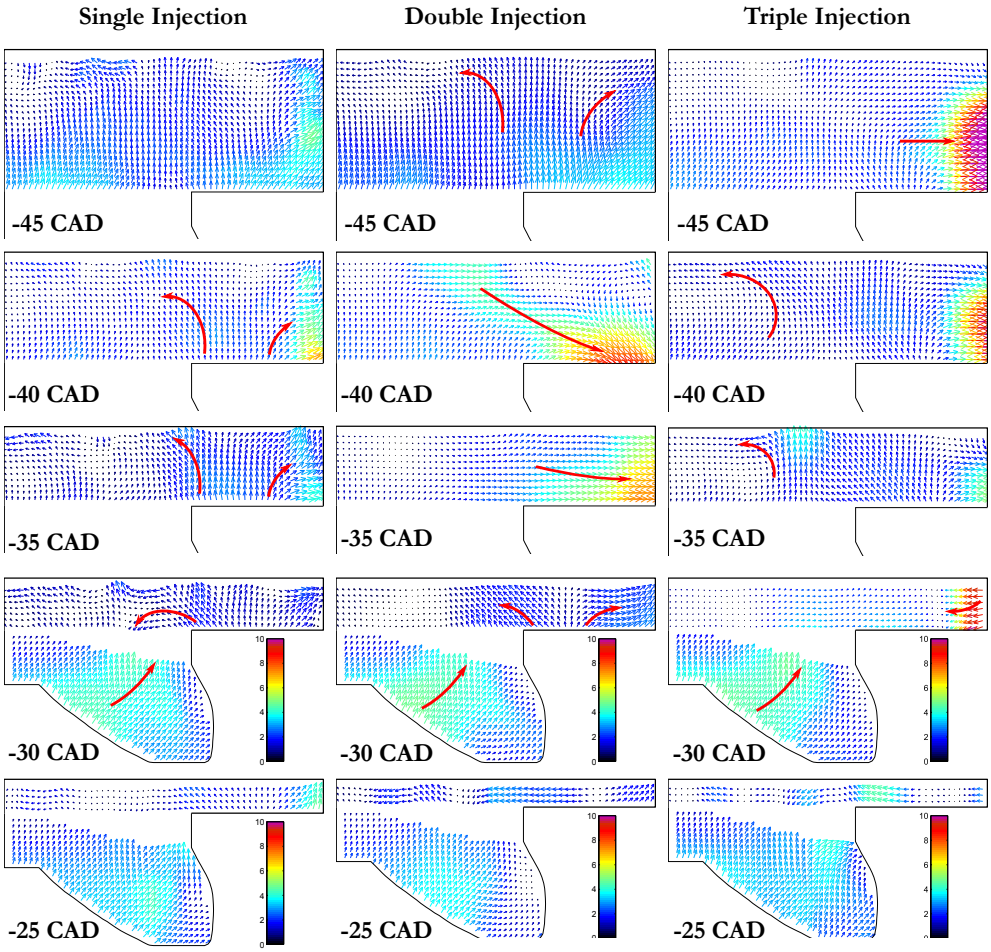

Figure 4.5: Mean flow field during compression phase for single, double and triple injection. The color bar illustrates the velocities in m/s.

Fuel injection phase

In-cylinder bulk motion coupled with the fuel injection process from -20 CAD to TDC are depicted in Figure 4.6. The source of the mean flow structures in the bowl at -20 CAD aTDC are primarily governed by the piston motion for all injection cases. The PIV results for the single injection case at -15 CAD aTDC indicate the profound influence of the injection process on in-cylinder flow structures. Deflection of the spray by the wall of the combustion chamber results in formation of an energetic, clockwise-rotating flow structure within the vertical measurement plane. However, this single rotating vortex is

primarily driven by the large source of linear momentum of the fuel jet and subsequently by the squish flow. Since the swirl number is sufficiently high (Rs = 2.6) and the centrifugal force on the fluid particle is increased [23], the squish flow will seek greater radii below the lip of the piston bowl and contribute to creating a strong vortex motion. At the highest swirl ratio, the flow structure in the bowl consists of a single vortex which is clearly visible up to TDC. Some fraction of the energy of the fuel jet can thereby be stored in the coherent mean flow and potentially be released later in the cycle as turbulent kinetic energy. This well-organized bulk flow structures not only transports fuel and fresh air to the same region, but also generates intense turbulence and enhances the small scale mixing at the fuel/air interface.

The last fuel injection events of the double and triple injection cases have shorter duration and are used primarily to trigger the combustion of the premixed fuel-air mixture. For this reason, the energizing times of the split injections are shorter compared to a single injection and the corresponding fuel jets have weaker linear momentum. As a consequent of the shorter fuel injection durations, the inward and upward displacement of the vortex position is reduced. In case of triple of injection, the central point of the vortex is mainly located down in the bowl.

Another feature to note in Figure 4.6 are the high velocities along the piston slope from -5 CAD aTDC to TDC for all three cases. This production of high velocities and their corresponding kinetic turbulence are associated with spray-wall interaction. Due to the high momentum of the fuel, the fluid elements from the outer region are redirected along the combustion chamber towards the inner region of the bowl where it encounters the quiescent flow (low-momentum) at the piston tip. Once the air and fuel are sufficiently mixed, the mixture is combustible.

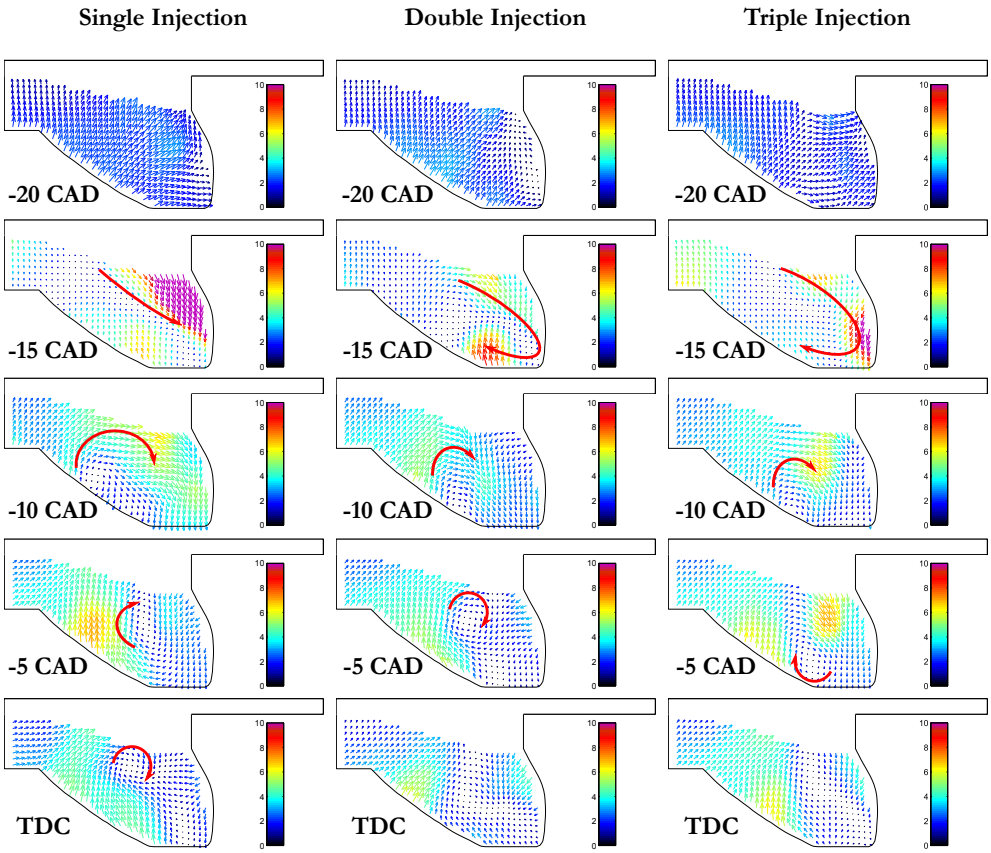

Figure 4.6: Mean flow field during injection phase for single, double and triple injection. The color bar illustrates the velocities in m/s.

Combustion and expansion phase

As the cycle proceeds, the vortex structure at 5 CAD aTDC starts to break down. Due to the combustion event and the ascending piston motion, an intense upward and downward fluid motion during heat release (5 and 10 CAD aTDC) is observed for all injection cases. Combustion is already well established following autoignition of the fuel leading to an increase in bulk gas temperatures and combustion-induced expansion, which causes velocity fluctuation within the piston bowl. Therefore, it is difficult to identify consistent bulk flow structure for all injection cases. The influence of combustion induced turbulence are described in section 4.3.

At 15 CAD aTDC, a considerable part of the squish volume becomes visible again. After the end of combustion, the flow at the piston lip spreads into the squish volume. Simultan-

eously, the piston drags the bulk flow downward between the piston top and the cylinder head, and mean velocities increases as the piston velocity increases. As the distance increases, a dominant clockwise-rotating vortex above the piston top begins to take shape. Additionally, a counter-rotating vortex above the bowl opening is formed in late expansion cycle. These coherent flow structures are a very common feature of engine flows, formed at the piston bowl mouth by hot oxidation products leaving the bowl. From optical studies [95], a zone of high soot/fuel concentration is observed at the location of clockwise-rotating vortex just above the piston top near the bowl rim. Late in the cycle, these structures transport also reaming unburned fuel into the squish volume and become trapped where quenching prevents subsequent oxidation.

Another interesting feature during expansion is the absence of radially flow in the squish volume and near the cylinder centreline. This lack of flow structure near the injector tip to facilitate transport and mixing are preferred zones of CO and *UHC* emissions. In [96, 97] also the authors show, a fuel vapour cloud forms at 30°CA around the injector tip as the sac volume dribble evaporates.

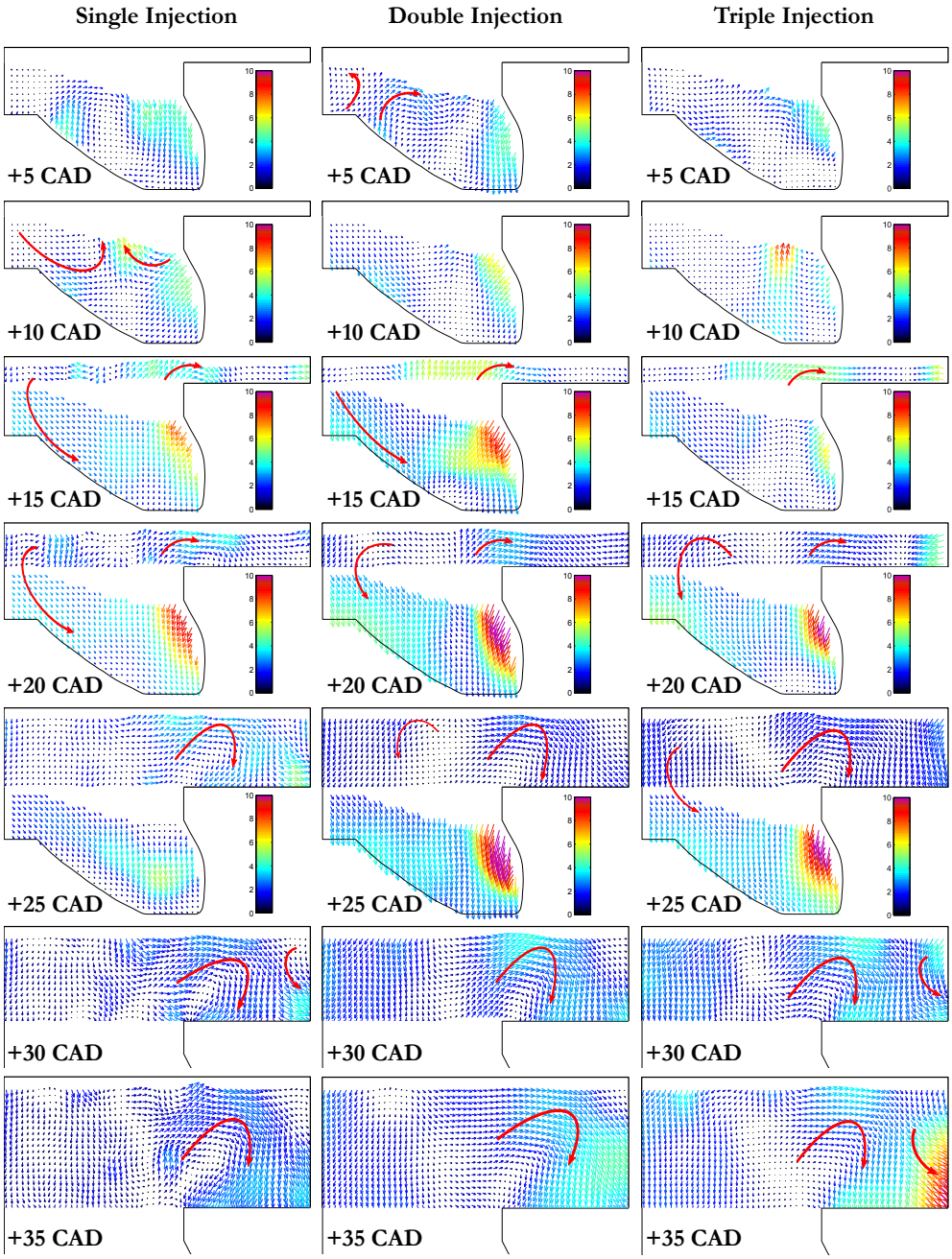

Figure 4.7: Mean flow field during expansion phase for single, double and triple injection. The color bar illustrates the velocities in m/s.

4.3 Spatial and time-resolved turbulence under PPC conditions

Another important aspect of this work cast light on the turbulence generation mechanisms under PPC conditions. This is based on Papers II and VI. In this section, the main focus is on the effects of multiple injection strategies on temporal and spatial turbulence evolution. Furthermore, analysis of wall-heat transfer based on the PIV data are presented.

4.3.1 Effects of split injections on Turbulent Kinetic Energy (TKE)

The kinetic energy introduced by the fuel injection event and rapid combustion of the fuel and air can explain the observed deviations in velocity profiles in the PIV measurement plane in section 4.2.1. In Paper II the spatial TKE was calculated and computed using equation 3.12. The way in which the combustion proceeds across the combustion chamber depends in great manner on the turbulence and the large-scale (coherent) motions.

Figure 4.8 shows the distribution of TKE for single and multiple injections events. Clearly, it is difficult to maintain high levels of turbulence during the expansion stroke. At this stage, the turbulence is strongly suppressed, and the mixing largely dependent on the piston speed and the coherent motion introduced during IVO. The distribution of TKE is approximately homogeneous, with the energy roughly equally distributed across the piston bowl. The computed TKE distribution during compression phase (-20 CAD aTDC), the triple injection indicates higher TKE areas close to piston pip compared to the single and double injection cases. This can be explained by the early fuel injections generating turbulence and that is not dissipating as rapidly as that obtained with double injection.

The second column in this figure illustrates the effect of fuel injection on TKE. After fuel is injected with 600 bar the bulk flow changes due to the associated high injection momentum of the fuel. Simultaneously, high TKE regions are discovered below the piston lip, where the spray gradually penetrates along the bowl surface at the outer radius. As seen in Figure 4.6, deflection of the fuel jets by the walls of the combustion chamber results in energetic rotating flow structures. Its is clearly visible that the fuel jet itself is a dominant source of turbulence and contributes to both the transport of fuel and air to a common interface and mixing them there. Furthermore, the scaling of the color bar indicates that TKE is pronounced also for the single injection case. The main reason is coupled to the injector energizing time. With a shorter duration of the second and third fuel injections, less fuel per injection enters the combustion chamber and turbulent mixing is consequently reduced.

The last column illustrates the combustion timings during the power-stroke. The single injection case is showing the highest TKE values both because of the high radial momentum stored in the fuel jet and the combustion-associated turbulence generation at peak heat

release (6 CAD aTDC). Measurements of TKE for the double and triple injection cases indicate a more spatially uniform energy distribution within the piston bowl. Studies in paper I on combustion stratification showed that the combustion following double or triple injections is more homogeneous than that of single injections. The injection strategy can thereby be used to control the excessive fuel stratification. It is relevant to note here that the peak heat release is at TDC for triple injection. By this time, the organized fluid motion is squeezed out of the squish volume and breaks up into turbulence and increases the turbulence level [14, 6].

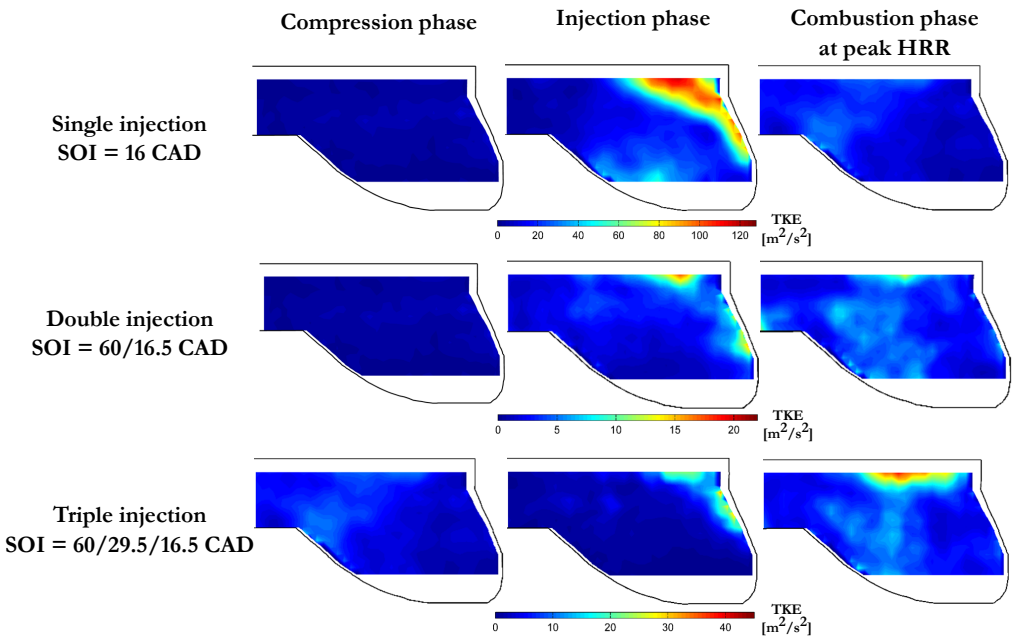

Figure 4.8: Global turbulent kinetic energy TKE distribution within the piston bowl.

In order to analyse the evolution of turbulence through the engine cycle, cycle-resolved turbulence was averaged over 44 instantaneous velocity fields at every second crank angle degree from -20 to 20 CAD aTDC. The complementary turbulence level for the different injection cases and motored condition are presented in Figure 4.9. As expected, motored engine operation gives a flat behaviour for the turbulence. During motored conditions the fluid motion in the piston bowl is entirely governed by the piston speed, which constitutes the only source of turbulence with low radial momentum. At first glance, the elevated turbulence for all injection cases are showing two visible peaks. As mentioned in section 4.3 the high injection momentum of the fuel leads to an increase in turbulence. Accordingly, the second peak is not caused directly by the fuel injection process or the flow structures it creates. It can be identified as turbulence generated by rapid gas expansion during the premixed combustion.

When comparing the three injection events, a single injection gives a higher turbulence level than double or triple injections. Especially the single injection event which releases the total fuel amount at -16 CAD aTDC leads to a steep increase in turbulence throughout the combustion process. When the main heat release starts at TDC, high velocities inside the bulk produces higher vorticity and turbulence. Considering further that turbulence is sharply suppressed during the expansion stroke and that very little turbulence is generated during the exhaust stroke, the turbulence at the end of the compression phase is determined primarily by the intake and the compression phases.

Another interesting effect to highlight is an increase in turbulence (3 m/s) for the triple injection case between -20 and -15 CAD aTDC. This increase in turbulence is mainly dominated by the fluid momentum carried from the second and third fuel injection, namely at -29.5 and -62.5 CAD aTDC. Since the time between the first and second injection for the double injection case is very large, the injection generated turbulence (at -62.5 CAD aTDC) breaks up and dissipates quickly.

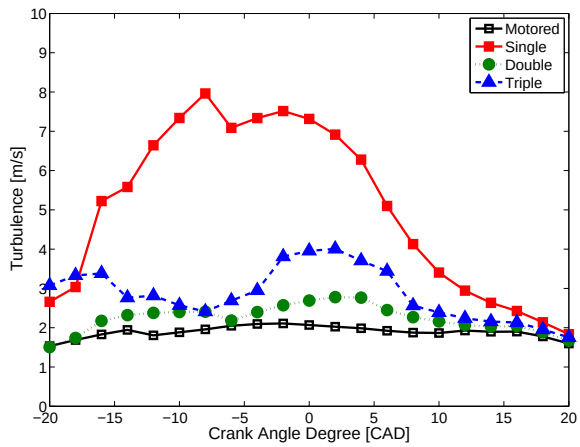

Figure 4.9: Global turbulent kinetic energy TKE distribution within the piston bowl.

4.3.2 Effects of TKE on heat transfer coefficient

In Paper 6, a particular methodology has been developed to comprehensively analyze spatial and temporal evolution of TKE and their effects on wall heat transfer coefficient. The primary focus of this study is to analyze PPC heat transfer associated to the velocities derived from PIV measurements. For that purpose, the Woschni model was modified in terms of the average piston speed. In this study, average piston speed is replaced by the characteristic velocity , which is calculated as follows Eq.4.1 and :

$$V_c(\theta) = \sqrt{{V_{\text{module}}}^2(\theta) + {V_{\text{tang}}}^2(\theta) + 2\overline{TKE}(\theta)} \tag{4.1}$$

$$V_{\text{module}} = \sqrt{{U_{\text{EA}}}^2 + {V_{\text{EA}}}^2} \tag{4.2}$$

Magnitudes for V_{module} and TKE are derived from the PIV measurements and averaged over a layer with thickness equal to 5% of the characteristic length of the bowl (maximum radius of the bowl for this study) [98]. The velocities of the three dimensional fluid consists beside the radial (v) and axial (u) components of the third tangential velocity ($v_{tangential}$). In that sense, the average evolution of this component is predicted by means of a 1D model [99].

As explained above, the global turbulence in Figure 4.9 was calculated by averaging the entire TKE plots (without dividing the combustion chamber in narrow zones). Figure 4.10 gives an example of the new approach used to determine TKE which is averaged along the axial direction as indicated with white dashed arrows. The averaged TKE is plotted at the bottom of the figure where 0 and 1 mark the bowl center and periphery, respectively. TKE has been normalized by the maximum value in the domain. Following this, a normalization allows for a more direct comparison of TKE spatial evolution under firing conditions. This procedure is further applied to all crank-angles at which PIV data is available, namely from -20 to 20 CAD aTDC.

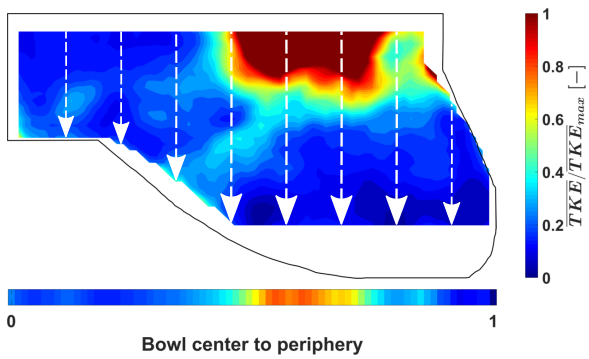

Figure 4.10: Normalized TKE at TDC under motored condition.

Normalized mean TKE plots for the same three injection cases as described above are then rearranged as shown in Figure 4.11. Each column shows the spatial distributions of normalized TKE averaged along the axial direction. Additionally, the wall heat transfer coefficients (Δh) are plotted with black dashed lines in relation to the motored case.

To explore the effects of injection and combustion on the flow field, TKE fields for different injection patterns have been normalized and subtracted by the motored TKE field. This method isolates contributions of injection and combustion allowing for a more suitable comparison. Dotted lines represent the injection event and dashed lines are used as a marker for the combustion duration.

The results for the spatial and temporal evolution connected with the injection strategies are shown in Figure 4.11. In terms of spatial TKE distribution, the single injection event places the gas with the highest tangential velocity near the bowl periphery by introducing high TKE. As explained in section 4.2.1, after fuel injection the spray has entrained bulk gas and transported it to the mid-bowl region (top image in Figure 4.11). This transport sets up a vertical vortex, which displaces the high velocity gas towards the center, maximizing the convective heat losses in this region [100]. Furthermore, it is clear that during the combustion duration, the TKE zones still remain in the central bowl region until it finally dissipates after 8 CAD aTDC.

The response of in-cylinder TKE fields to double and triple injection strategies were also evaluated. The first observation for these strategies is that, when comparing them to each other, their spatial TKE distributions follow a similar trend. Both are showing low TKE fields around the bowl center between EOI and CA10 (dotted and dashed lines). As expected, the last short fuel injection pulse, under double and triple injection strategies, introduces lower TKE levels in which the spray is redirected along the piston wall towards the bowl centre. By contrast, high TKE is located near the periphery and moderate TKE levels closer to the bowl centre, while the central zone gives lower TKE intensity values. This last observation differs from what was observed with a single fuel injection was occurred. Regarding combustion, it again mainly influences central bowl region and it is dissipating when combustion process is over.

Finally, it is evident that of the temporal evolution wall heat transfer coefficient is strongly influenced by the injection pattern. Black dashed lines show wall heat transfer coefficient differences in comparison to the motored case. The top of Figure 4.11 shows how the single injection case differs the most with respect to the reference case. Both injection and combustion processes induce sharp raises. It is noticeable that the heat transfer coefficient after EOI remains close to the level reached at EOI. However, the combustion peak at 4 CAD aTDC is followed by a continuous drop.

For the multiple injection cases, the pilot injections result in a positive effect on the heat coefficient. Due to better mixing of fuel and air, a thermally stratified charge can appear. Further, Δh for double and triple injection strategies follws the motored condition to a great extent during compression phase. As for combustion, just after -4 CAD aTDC, the wall heat transfer coefficient for the triple injection pattern shows a slightly sharper increase in comparison to the double injection case. However, longer combustion durations (multiple

injection cases) lead to smoother temporal evolutions of Δh and lower peak values compared to the single injection case.

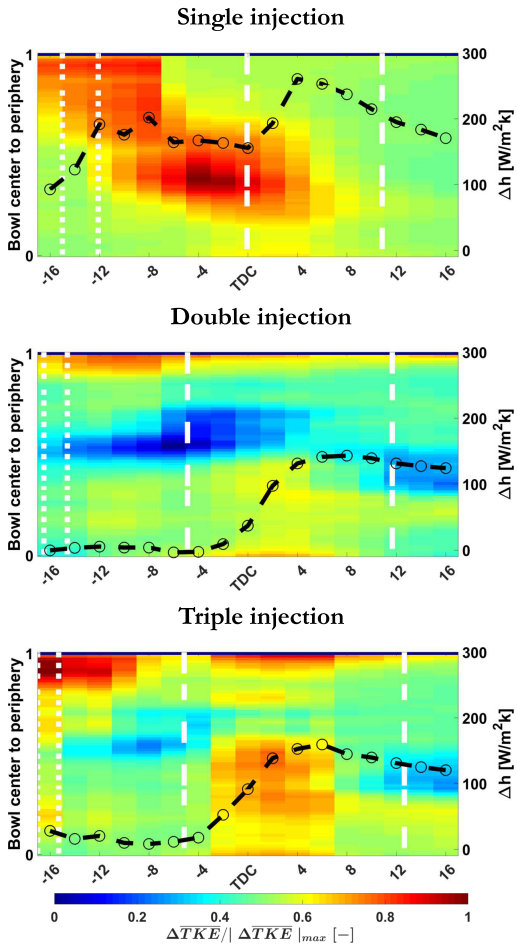

Figure 4.11: Spatial and temporal evolution of normalized ΔTKE. Additionally, black dashed lines illustrate the temporal evolution of heat transfer coefficient Δ h. The Figures from top to bottom illustrate: single, double and triple injection cases.

4.4 Cyclic variation

In-cylinder cyclic variability is caused by large-scale (coherent flow) variations from random turbulent flow structures which effects the gas motion and combustion throughout the cylinder [101]. Methods to identify and separate measured velocity fluctuations due to these two sources typically rely on temporal or spatial filtering techniques. As explained

in section 3.3.2, specific tools have been developed to accomplish this, including proper orthogonal decomposition (POD). This technique expresses the flow structure in terms of orthogonal basis functions, also known as the POD-modes, which capture the highest flow energy using the fewest modes.

The main objective of this section is to analyze the cyclic variability based on the acquisition of several snapshots at each crank-angle position over 44 cycles, on which a POD analysis is then performed and quantified. Figure 4.12 presents the energy fraction as a function of the mode number. Each of the presented curves correspond to different CAD positions: case 1 represents the late phase of compression stroke, case 2 the combustion phase and case 3 the expansion stroke. The first observation that can be made from Figure 4.12 is that the first modes (lowest mode number) contains the highest kinetic energy and for higher mode numbers, the curves for case 1 and case 3 show a steep decrease compared to case 2. In principle, this high energy fraction in the first POD mode indicates a highly organized flow with small cycle-to-cycle variations. In contrast, case 2 captures only 29% of the energy fraction in the first mode as a result of the heat release at this CAD position. This implies that the flow during combustion (case 2) varies considerably from cycle to cycle, and that the flow is relatively disorganized. In principle, about 80% of the kinetic energy is contained in the first 5 modes for case 1 and case 2, and for case 3 a larger set of modes is required to obtain a good level of similarity with the original field.

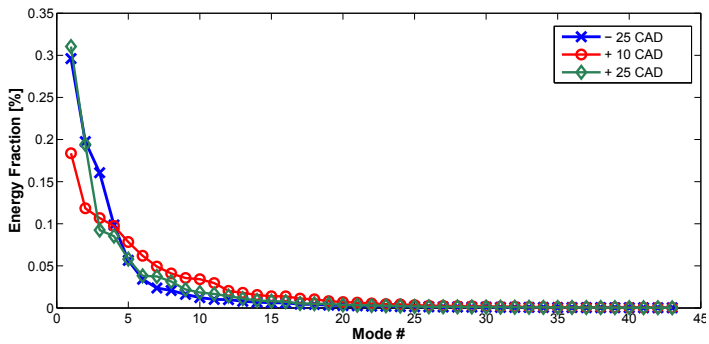

Figure 4.12: Normalized energy fraction as a function of the POD mode numbers for different CAD positions.

As discussed earlier, the POD coefficients are obtained by projecting the POD modes onto the original velocity fields. For snapshot POD, this gives a time-varying coefficient for each mode. It should be noted that if the cycle-to-cycle variability is zero,the value of $a(i)$ (*Eq*. 3.16) for a particular mode M will always appear constant. The magnitude of variation of $a(i)$ at a given piston position is an indication of the cycle-to-cycle variations, and this can be quantified by computing the standard deviation in $a(i)$ at each piston position using the first mode.

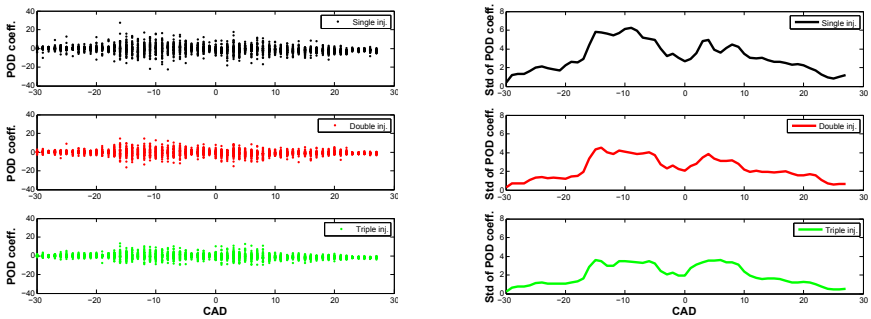

(**a**) POD coefficients of first mode for single, double and triple injection. At each CAD, 44 coefficients illustrate the variation among the 44 cycles.

(**b**) Standard deviation of the coefficients over 44 cycles.

Figure 4.13: Temporal coefficients variations from 2D phase-invariant POD.

Figure 4.13.*a* demonstrates the fluctuation of the POD coefficients at every CA for the temporal resolution from -30 to 30 CAD aTDC for single, double and triple injection. The spread in the coefficient values over the 44 instantaneous frames is greatest around -15 and 10 CAD aTDC. The degree of the spread is quantified by calculating the standard deviation in the coefficient value at each phase. This method is based on the work outlined in [102], a quantitative index for cycle-to-cycle as a function of crank-angle degrees is derived and computed in figure 4.13.b.

As visible in the graphs, the reported modes present essentially two peaks of fluctuations (4.13.b). The first peak corresponds to the fuel injection. From the PIV data in 4.2.1 we have obtained an organized flow until the first or last fuel injection. After fuel is injected into the piston bowl, the well-organized flow begins to change and forms a clockwise rotating vortex, causing an increase in the standard deviation of the POD coefficient. Later the in-cylinder flows begin to stabilize until the fuel-air mixture auto-ignites. The heat release that follows,s indicates again an increase in the standard deviation of the POD coefficient. This second peak is a potential sources of the high cycle-to-cycle variations with disorganized flow. For single injection case, the cycles are varying significantly in contrast to those with double and triple injection, whereas the combustion-induced variations are not significant. A coherent flow field appears after the combustion, indicating that the coefficients are decreasing during the expansion stroke.

4.5 Combustion and emission characteristics of gasoline- PPC with small quantities of ethanol

In this work PPC (or GCI) was operated using gasoline blended with small quantities of ethanol (30 vol %). EGR was swept from $0 - 28\%$ at three different λ rates.

Figure 4.14 shows a comparison of the RoHR profiles obtained at various λ levels for double injection strategies with a split ratio of 50 : 50. The first fuel event is placed at -50 CAD aTDC, while the second fuel injection was optimized in order to achieve a constant CA50 (4 CAD aTDC) while introducing cooled EGR into the engine. Splitting the fuel into two injection pulses create a more uniform air-fuel distribution inside the cylinder before the start of combustion. As clearly seen in Figure 4.14, several observations can be drawn on the different combustion characterizations. Focusing on the air-fuel equivalence ratio (λ) there is a clear trend for the RoHR shapes. Reducing λ leads to a clearly visible staged combustion characteristics for EGR contents below 10%. The first peak in the RoHR comes from the first fuel injection in which the premixed charge autoignites just before TDC. With long ignition delay, the mixture packets where combustion takes place and gradually proceeds will be near the global mixture strength. The fuel introduced from the second injection enters the premixed combustion zone from the first injection and is likely to result in stratified combustion with a noticeable change in the shape of the RoHR (an associated second peak following a longer combustion tail).

The second observation concerns the EGR effect on the heat release profiles. For $\lambda = 2$ operation the EGR rate has less effect on the RoHR and gives a single-stage heat release profile with small variations in the peak values. For richer conditions, an increase in EGR transformed the shape of the RoHR from a double-staged combustion to a single-stage profile with a higher peak, as can be seen for cases with 20% and 25%EGR. High EGR levels prevents the fuel from first injection to react, while the second fuel injections triggers the combustion by achieving the right global and local mixture strength.

Since increasing EGR delayed autoignition, the combustion phasing was kept constant at 4 CAD aTDC by advancing the timing of the second fuel injection (SOI_2), as presented in Figure 4.15.a. Thus, the second fuel injection was the main parameter to control the correct combustion phasing for a fixed EGR level and global air-fuel equivalence ratio. Leaner in-cylinder conditions with higher EGR levels lead to a separation of few a degrees between the last injection and start of combustion. This promotes mixing for the last fuel injection. Secondly, Figure 4.15.b shows CA10 as a function of EGR level. CA10 follows the trend already shown in the RoHR, becoming retarded when decreasing the EGR level from 25 towards 0 and switching from lean to rich mixture. The use of cooled EGR helped to slightly retard CA10 in most of the points, except for the $\lambda = 2$ condition where it varies within a narrow CA window. Thirdly, another important combustion parameter for

PPC combustion is the increased combustion noise (Figure 4.15).c due to the increased premixing compared to the $\lambda = 1.8$ and $\lambda = 1.6$ conditions. For the leanest mixture condition, $\lambda = 2$, the premixed charge exhibits a sharp auto-ignition process followed by a fast combustion, which is similar to knocking and thus causes high combustion noise. It is also worth to remark that, if combustion noise is compared, higher EGR presents noise levels above 90 dB.

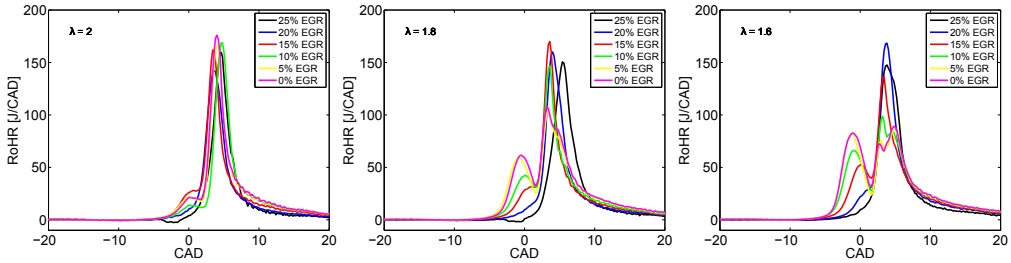

Figure 4.14: Effects of EGR on combustion characteristics for various air-fuel equivalence ratios (λ).

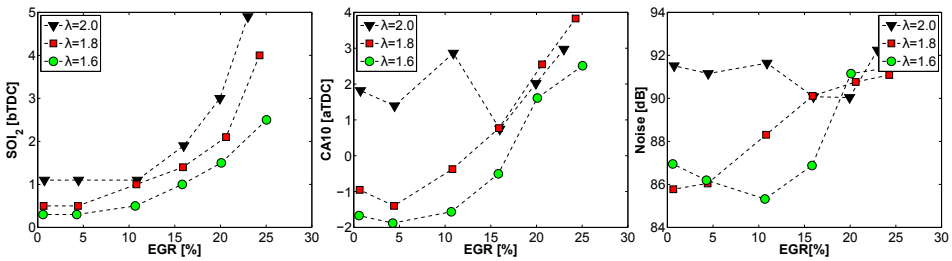

(a) Second fuel injection as a function of EGR.

(b) CA10 as a function of EGR.

(c) Combustion noise vs EGR

Figure 4.15: Effects of EGR onlast fuel injection, CA10 and combustion noise for various air-fuel equivalence ratios (λ).

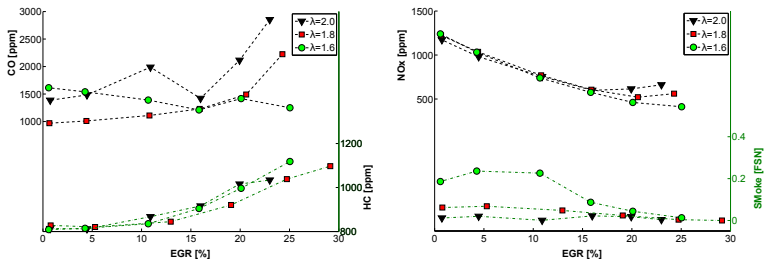

(a) CO and unburned HC emissions as a function of EGR.

(b) NO_x and smoke vs EGR

Figure 4.16: Effects of EGR on last fuel injection timing, CA10 and combustion noise for various air-fuel equivalence ratios (λ).

Focusing on exhaust emissions, Figure 4.16 a) and b) summarizes the main trends for *CO*, *UHC*, NO_x and smoke emissions when increasing the EGR rate for different air-fuel ratios. Both *CO* and *UHC* consequently increase with higher dilution ratios, which worsens the fuel energy conversion and oxidation processes. Another explanation can be due to the first fuel injection early in the compression stroke, in which liquid fuel penetrates in lower air temperature and density zones, risking impingement onto the cylinder surfaces may easily occur. However, *CO* formation at $\lambda = 1.6$ operation shows an unexpected decrease compared to the leaner operation conditions.

Figure 4.16.b reveals the effects of air-dilution over the NO_x and soot emissions. The experimental results corroborate how NO_x emissions are decreased for increased EGR rates. It is well known that the reduction in thermal NO_x formation during PPC operation is mainly attained by decreasing the peak combustion temperatures through the use of cooled high EGR rates. The smoke shows another interesting trend. It is surprisingly decreased when EGR is increased. It is well-known that NO_x and soot tend to have an inherent trade-off in CDC concepts (explained in Chapter 2). There, the main reason for suppressing smoke for higher EGR rates is the oxygenated fuel with ethanol content. Ethanol is an alcohol characterized by the hydroxyl OH group. The additional oxygen atom and high octane number within the fuel, helps avoiding fuel rich combustion and thus significantly reduces soot formation.

To complement the combustion analysis, the combustion process was visualized by means of an endoscopic system (AVL VisioScope). The 4th cylinder was modified in the cylinder head to gain optical access into the combustion chamber. The endoscopic setup consists of an endoscope probe with 70° mirror, a CCD camera (13.5 fps) to capture the flame luminosity and image processing software (ThermoVision) using the Two-Color- Method [81, 103, 104] to obtain crank angle resolved soot concentrations. Due to the low frame rate of the camera it was not possible to record the entire combustion event within a single engine cycle. Therefore, the images where taken as an integration of consecutive cycles to provide a complete combustion evolution. It was assumed that the combustion would be quite similar from cycle to cycle based on the low COV of IMEP (below 3%).

The integral soot concentration distribution for different EGR rates in the crank angle domain is presented in Figure 4.17. Any illuminated pixel on the camera is related to the soot value as integral soot concentration within the endoscope viewing area. A Gaussian fit was applied to the data set in order to gain clear trends. When the EGR level is increased from 0% to 25%, the peak soot value decreases significantly. EGR is a well-known leverage for in-cylinder temperature reduction and also for increasing the ignition delay. A longer ignition delay enables an enhanced fuel-air mixing to avoid locally fuel-rich regions. Besides that, the fuel itself contains also oxygen molecules which further contributes to the in-cylinder soot oxidation and reduces the reported soot values.

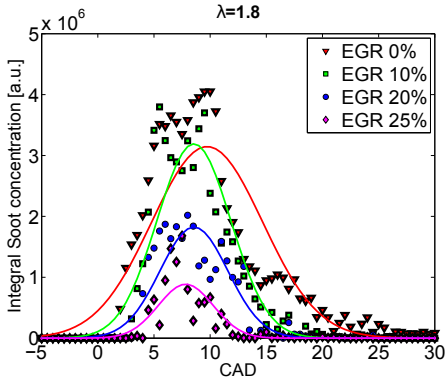

Figure 4.17: Image averaged soot concentrations calculated from AVL VisioScope data for three EGR levels (λ=1.8, Tin=55°C, Pin = 1.4 bar.

Figure 4.18 presents in-cylinder 2D images depicting the combustion process for $\lambda = 1.8$ operation for the cases with 0%, 10% and 20% EGR rates. Natural combustion luminosity is presented on the left-hand side and the spatial soot distribution to the right. As mentioned, the soot concentration is determined by the Two-Color-Method implemented in the commercial software and applied for every color pixel (from the RGB matrix) of the image field. The influence of EGR on combustion luminosity can be clearly observed in the endoscopic combustion images. It decreases significantly with an increase in EGR, due to the reduced in-cylinder combustion temperature. At 3 CAD aTDC in the case without EGR, the fuel penetration (from second injection) into the combustion zone can be observed easily with the naked-eye. Combustion clouds around the piston-pip are detected as the combustion proceeds during several crank angle degrees. This behaviour was also found in Figure 4.1. Furthermore, the influence of elevated EGR levels on soot concentration is depicted on right-hand in Figure 4.18. Bright regions in the contour indicates the presence of an optically thick soot cloud. However, the soot data indicate that the soot formation decreases with increased EGR when using gasoline fuel with 30% ethanol concentration. This is also consistent with the observations in Figure 4.17. A remarkable observation is the fast soot oxidation within 10 to 15 CAD for cases with 0% and 10% EGR. After 15 CAD aTDC and also during the entire combustion process with 20% EGR, no spatial soot distribution within the field of view is detected. The higher oxygen content of ethanol enabling longer ignition delay for premixing to avoid fuel rich zones. Another significant reason is, that the combustion occurs at temperatures below that needed to form soot [24].

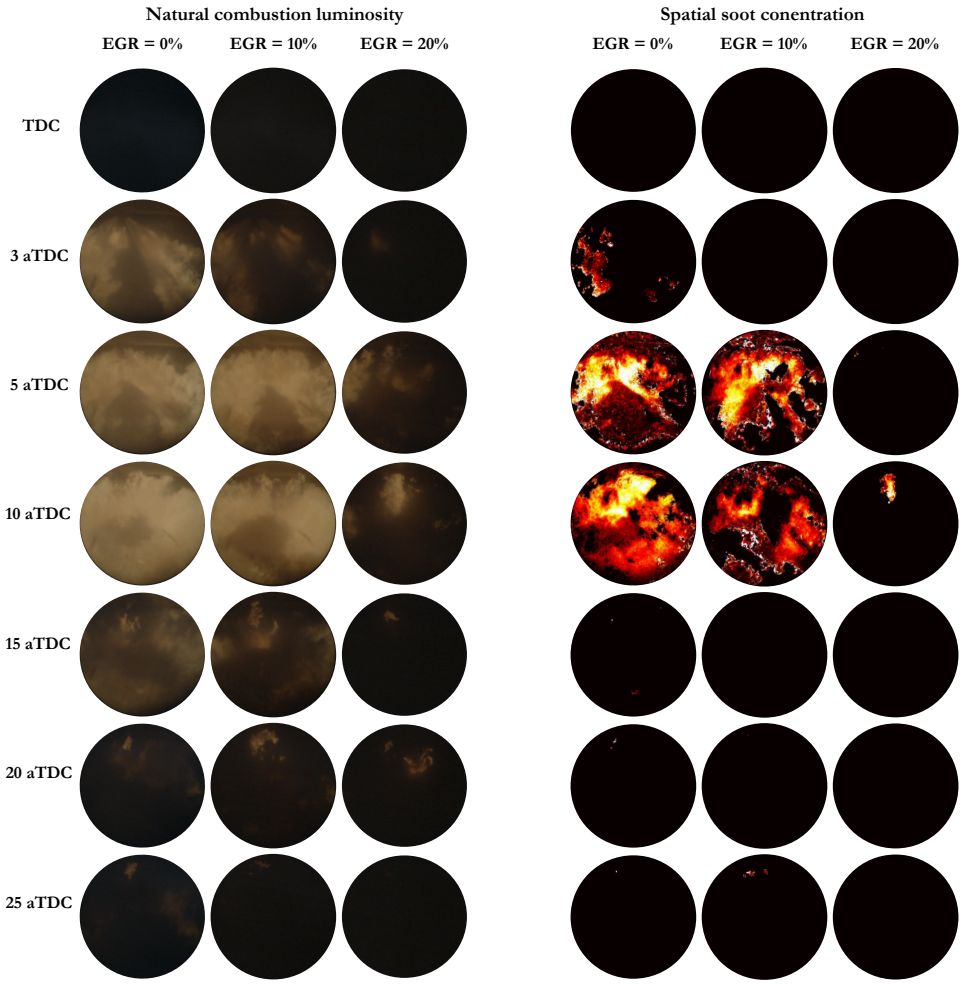

Figure 4.18: Endoscope images of gasoline E30 at various EGR levels (λ=1.8, Tin=55 °C, Pin = 1.4 bar).
Left hand-side: Luminosity images of the combustion sequence.
Right hand-side: Time-sequence of spatial soot distribution within the field-of-view.

CHAPTER 5

SUMMARY AND CONCLUSION

This research has focused on in-cylinder visualization of PPC using high octane fuels in a light-duty CI engine. The main objectives was to contribute to the understanding of the in-cylinder combustion process and the complex bulk-flow structures by examining the effects of different injection strategies.

5.1 Combustion stratification

In this work, the dominant controlling factor of the PPC process was investigated by conducting optical engine experiments to visualize the effect of injection events. For this first phase, the engine was equipped with a variable valve train to trap hot residuals, which helps to elevate the charge temperature to reach auto-ignition of a high-octane fuel (PRF70). The OH* chemiluminescence—a marker for high-temperature combustion—shows that ignition occurs in the outer region of the combustion chamber in small isolated pockets under light-load conditions. These ignition zones grow for several crank angle degrees while more ignition pockets continue to appear. The separate ignition pockets then merge into larger, more coherent reaction zones and steadily move back toward the center of the combustion chamber. These reaction zone movements appear to be governed by the occurrence of isolated auto-ignition pockets, rather than propagation of a continuous reaction zone. A new methodology was applied to analyse the stratification level of the reaction zones by using the chemiluminescence image data. The effects of single, double and triple injections were investigated, relating to the combustion stratification. The results indicate a significant decrease in stratification level when splitting the fuel in three individual injections during the

compression stroke. For the triple injection cases, the proportion of fuel injected during the first pulse is assumed to be completely vaporized and uniformly mixed with air. The second injection pulse leads to more fuel stratification of the charge and the last injection triggers the combustion after the fuel and air is sufficiently mixed during the compression stroke.

5.2 Experimental fluid dynamics

The second phase of the present work focuses on characterization of the main properties of the in-cylinder flow under PPC conditions by utilizing single, double, and triple injection strategies. In-cylinder, high-speed PIV experiments were successfully conducted for a production-type optical piston geometry. An extensive data set of velocity maps were acquired in the vertical measurement field. The density of seeding particles (TiO_2) was kept as low as possible to reduce window fouling and background light scattering from particles outside the measurement volume, and to reduce the risk of multiple particles in the measurement volume. Vector fields were acquired within the piston bowl and squish regions during the compression, injection, combustion, and expansion phases to highlight the flow and combustion interactions throughout an engine cycle and their effects on the turbulence production. In addition to the vector fields, heat-release analysis were used to improve the interpretation of the vector and turbulence maps.

The flow analysis given in Sections 4.2 and 4.3 showed insights into the temporal and spatial in-cylinder flow and turbulence structures for various injection strategies. A methodology was developed to generate maps with the temporal and spatial evolution of TKE. The wall heat transfer coefficient was also computed based on a modification of the empirical correlation proposed by Woschni [82]. The observed results showed an organized flow structure during compression phase. After this, introducing fuel into the combustion chamber lead to a dominant change in the flow structures and the turbulence level. Interactions of the jets with the bowl wall resulted in the formation of strong, clockwise-rotating vortex structures in the imaged plane within the piston bowl for all injection cases. Furthermore, the results also revealed a strong influence of heat release on the flow field, leading to disorganized flow patterns and high turbulence levels. Evaluation of the TKE plots during the combustion phase indicated a more spatially uniform energy distribution within the bowl compared to the single injection case. In contrast to this, a single fuel injection lead to higher TKE, initially located at the bowl periphery and gradually transported towards the bowl center. Alternatively, the temporal evolution of the wall heat transfer coefficient showed a strong influence from the injection and combustion processes. Especially for the single injection pattern, wall heat transfer (in reference to motored case) before the start of combustion was mainly driven by changes in the flow field. After the start of combustion, differences in in-cylinder thermodynamic conditions also contribute to reaching higher wall heat transfer

levels. For multiple injection patterns, the greatest differences in wall heat transfer (in reference to motored case) were observed after the start of combustion and were mainly driven by changes in the in-cylinder thermodynamic conditions. In addition to this, proper orthogonal decomposition (POD) was applied to extract cycle-to-cycle fluctuations of the flow field to evaluate only the turbulent data. The cycle-to-cycle flow variations were quantified using the standard deviation of the POD coefficients across the engine cycles. Although the results showed less fluctuation when coherent flow structures were present, the injection and combustion processes lead to a significant change in the flow field, giving rise to cyclic variations.

5.3 Influence of ethanol-gasoline blends on PPC

In the last phase, combustion and emission studies of the PCC concept were conducted in four-cylinder, 1.9-litre CI engine using E30 gasoline, which contains 30 percent ethanol. The experiments were coupled with endoscopic measurements. The main objective of this work was to use double injections to achieve low emissions and combustion noise at intermediate loads. The results present the influence of EGR and air-fuel ratio on the autoignition and combustion processes, as well as on the emission formation of the high-octane biofuel. Compared to regular diesel or gasoline PPC, E30 showed great improvements for both NOx and soot formation. Endoscopic imaging revealed that due to the longer premixing time and better air entrainment into the fuel jets, E30 PPC produced less soot.

5.4 Thesis contributions

This work presents an insight into how combustion stratification, fuel distribution and flow development affect PPC for different injection strategies in a compression ignition engine. The main contributions are listed below. The thesis shows, for the first time:

- How the injection strategy affects the fuel stratification level and the local fuel distribution prior to the start of combustion. The results demonstrated that redistribution of the fuel injection pulses leads into higher homogeneity of the premixed charge compared to a single injection strategy.
- How various injection timings and injection strategies change the bulk flow and squish flow. A detail description of ensemble average flow fields, the spatial and temporal turbulent kinetic energy development, and cyclic variation based on the flow fields under PPC conditions was presented.

- An experimental approach to calculate an experimental heat transfer coefficient based on velocity data has been presented under PPC conditions. It was demonstrated that for multiple injection strategies the wall heat transfer was reduced.
- Endoscopic investigation of various engine parameter (λ, EGR, SOI) on combustion emissions and efficiency under part load. In general, the results showed the emission of soot and NOx for gasoline-ethanol blend were low at PPC condition with moderate EGR levels.

CHAPTER 6

BIBLIOGRAPHY

[1] The Outlook for Energy: A View to 2040. Exxon Mobil Corporation, 2016.

[2] EU-27 Energy FLow 2006. http://www.sankey-diagrams.com/european-energy-flows-sankey/. Accessed: 2017-03-04.

[3] Daniel A Lashof and Dilip R Ahuja. Relative contributions of greenhouse gas emissions to global warming. Nature, 344(6266):529–531, 1990.

[4] NASA global climate change. https://climate.nasa.gov/causes/. Accessed: 2017-04-04.

[5] DieselNet emission standards. https://www.dieselnet.com/standards/. Accessed: 2017-04-04.

[6] John Heywood. Internal combustion engine fundamentals. McGraw-Hill Education, 1988.

[7] John E Dec. A conceptual model of DI diesel combustion based on laser-sheet imaging. SAE Technical Paper 970873, 1997.

[8] Dale R. Tree and Kenth I. Svensson. Soot processes in compression ignition engines. Prog. Energy Combust. Sci., 33(3):272–309, 2007.

[9] Irvin Glassman, Richard A Yetter, and Nick G Glumac. Combustion. Academic press, 2014.

[10] Sage Lucas Kokjohn. Reactivity controlled compression ignition (RCCI) combustion. PhD thesis, 2012.

[11] Yuzo Aoyagi, Takeyuki Kamimoto, Yukio Matsui, and Shin Matsuoka. A gas sampling study on the formation processes of soot and NO in a DI diesel engine. Technical report, 1980.

[12] Takeyuki Kamimoto and Myurng-hoan Bae. High combustion temperature for the reduction of particulate in diesel engines. Technical report, 1988.

[13] Gary D Neely, Shizuo Sasaki, Yiqun Huang, Jeffrey A Leet, and Daniel W Stewart. New diesel emission control strategy to meet US Tier 2 emissions regulations. SAE Technical Paper 2005-01-1091, 2005.

[14] John L Lumley. Engines: an introduction. Cambridge University Press, 1999.

[15] Tarek Echekki and Epaminondas Mastorakos. Turbulent combustion modeling: Advances, new trends and perspectives, volume 95. Springer Science & Business Media, 2010.

[16] Jean Rabault. PIV Investigation of the Intake Flow in a Parallel Valves Diesel Engine Cylinder, 2015.

[17] A D Gosman. Flow processes in cylinders. Thermodynamics and gas dynamics of internal combustion engines, 2:617–772, 1986.

[18] Sherif H E I Tahry. A numerical study on the effects of fluid motion at inlet-valve closure on subsequent fluid motion in a motored engine. Technical report, 1982.

[19] Constantine Arcoumanis and Take Kamimoto. Flow and combustion in reciprocating engines. Springer Science & Business Media, 2009.

[20] Paul C Miles, Bret H Rempelewert, and Rolf D Reitz. Squish-Swirl and Injection-Swirl Interaction in Direct-Injection Diesel Engines.

[21] P Miles, M Megerle, J Hammer, Z Nagel, R Reitz, and V Sick. Late-cycle turbulence generation in swirl-supported, direct-injection diesel engines. SAE 2002 World Congress, (724), 2002.

[22] P Miles, M Megerle, Z Nagel, R Reitz, Ming-Chia D Lai, and V Sick. An experimental assessment of turbulence production, Reynolds stress and length scale (dissipation) modeling in a swirl-supported DI Diesel Engine. SAE 2003 World Congress, 2003.

[23] Paul C Miles, Bret H Rempelewert, and Rolf D Reitz. Squish-Swirl and Injection-Swirl Interaction in Direct-Injection Diesel Engines.

[24] Kazuhiro Akihama, Yoshiki Takatori, Kazuhisa Inagaki, Shizuo Sasaki, and Anthony M Dean. Mechanism of the smokeless rich diesel combustion by reducing temperature. SAE technical paper 2001-01-0655, 2001.

[25] J V Pastor, J M García-Oliver, A García, C Micó, and R Durrett. A spectroscopy study of gasoline partially premixed compression ignition spark assisted combustion. Applied Energy, 104:568–575, 2013.

[26] Jesus Benajes, Bernardo Tormos, Antonio Garcia, and Javier Monsalve-Serrano. Impact of Spark Assistance and Multiple Injections on Gasoline PPC Light Load. SAE International Journal of Engines, 7(4):2014–01–2669, 2014.

[27] Hakan Persson, Johan Sit, Elias Kristensson, and Bengt Johansson. Study of Fuel Stratification on SparkAssisted Compression Ignition (SACl) Combustion with Ethanol Using High Speed Fuel PLIF Study of Fuel Stratification on Spark Assisted Compression Ignition (SACl) Combustion with Ethanol Using High Speed Fuel PLIF. (724):776–790, 2008.

[28] Robert John Middleton. Simulation of spark assisted compression ignition combustion under EGR dilute engine operating conditions. PhD thesis, 2014.

[29] Vinod K Natarajan, Volker Sick, David L Reuss, and Gerald Silvas. Effect of spark-ignition on combustion periods during spark-assisted compression ignition. Combustion Science and Technology, 181(9):1187–1206, 2009.

[30] Ida Truedsson. The HCCI Fuel Number - Measuring and Describing Auto-ignition for HCCI Combustion Engines. PhD thesis, Lund University, 2014.

[31] Yoshinaka Takeda, Nakagome Keiichi, and Niimura Keiichi. Emission characteristics of premixed lean diesel combustion with extremely early staged fuel injection. Technical report, 1996.

[32] Thomas W Ryan and Timothy J Callahan. Homogeneous charge compression ignition of diesel fuel. Technical report, 1996.

[33] Hisashi Akagawa, Takeshi Miyamoto, Akira Harada, Satoru Sasaki, Naoki Shimazaki, Takeshi Hashizume, and Kinji Tsujimura. Approaches to solve problems of the premixed lean diesel combustion. Technical report, SAE technical Paper, 1999.

[34] John E Dec and Magnus Sjöberg. A parametric study of hcci combustion-the sources of emissions at low loads and the effects of gdi fuel injection. Technical report, SAE Technical Paper, 2003.

[35] Magnus Sjöberg, John E Dec, and Nicholas P Cernansky. Potential of thermal stratification and combustion retard for reducing pressure-rise rates in hcci engines, based on multi-zone modeling and experiments. Technical report, SAE Technical Paper, 2005.

[36] Bruno Walter and Bertrand Gatellier. Development of the high power NADI™ concept using dual mode diesel combustion to achieve zero NOx and particulate emissions. Technical report, 2002.

[37] Shigeru Onishi, Souk Hong Jo, Katsuji Shoda, Pan Do Jo, and Satoshi Kato. Active thermo-atmosphere combustion (ATAC)-a new combustion process for internal combustion engines. SAE Technical Paper 790501, 1979.

[38] Robert H Thring. Homogeneous-charge compression-ignition (hcci) engines. Technical report, SAE Technical paper, 1989.

[39] Paul M Najt and David E Foster. Compression-ignited homogeneous charge combustion. Technical report, 1983.

[40] Yoshinori Iwabuchi, Kenji Kawai, Takeshi Shoji, and Yoshinaka Takeda. Trial of new concept diesel combustion system-premixed compression-ignited combustion. Technical report, 1999.

[41] Magnus Christensen and Bengt Johansson. Supercharged homogeneous charge compression ignition (HCCI) with exhaust gas recirculation and pilot fuel. Technical report, 2000.

[42] John E Dec and Yi Yang. Boosted HCCI for high power without engine knock and with ultra-low NOx emissions-using conventional gasoline. SAE International Journal of Engines, 3(2010-01-1086):750–767, 2010.

[43] F Foucher, P Higelin, C Mouna□m-Rousselle, and P Dagaut. Influence of ozone on the combustion of n-heptane in a HCCI engine. Proceedings of the Combustion Institute, 34(2):3005–3012, 2013.

[44] Shuji Kimura, Osamu Aoki, Hiroshi Ogawa, Shigeo Muranaka, and Yoshiteru Enomoto. New combustion concept for ultra-clean and high-efficiency small DI diesel engines. SAE Technical Paper 1999-01-3681, 1999.

[45] Shuji Kimura, Osamu Aoki, Yasuhisa Kitahara, and Eiji Aiyoshizawa. Ultra-clean combustion technology combining a low-temperature and premixed combustion concept for meeting future emission standards. SAE Technical Paper 2001-01-0200, 2001.

[46] Keiji Kawamoto, Takashi Araki, Motohiro Shinzawa, Shuji Kimura, Shunichi Koide, and Masahiko Shibuya. Combination of combustion concept and fuel property for ultra-clean DI diesel. Technical report, 2004.

[47] Miles and P.C. Rate-Limiting Processes in Late-Injection, Low-Temperature Diesel Combustion Regimes, in Proc. page 18, 2004.

[48] Ryo Hasegawa and Hiromichi Yanagihara. HCCI combustion in DI diesel engine. volume 2003. SAE Technical Paper 2003-01-0745, 2003.

[49] Kazuhisa Inagaki, Takayuki Fuyuto, Kazuaki Nishikawa, Kiyomi Nakakita, and Ichiro Sakata. Dual-fuel PCI combustion controlled by in-cylinder stratification of ignitability. Technical report, 2006.

[50] Derek A Splitter. High efficiency RCCI combustion Doctor of Philosophy University of Wisconsin – Madison. (January 2012), 2012.

[51] Sage L Kokjohn, Mark P B Musculus, and Rolf D Reitz. Evaluating temperature and fuel stratification for heat-release rate control in a reactivity-controlled compression-ignition engine using optical diagnostics and chemical kinetics modeling. Combustion and Flame, 162(6):2729–2742, 2015.

[52] David T Klos and Sage L Kokjohn. Investigation of the Effect of Injection and Control Strategies on Combustion Instability in Reactivity-Controlled Compression Ignition Engines. Journal of Engineering for Gas Turbines and Power, 138(1):11502, 2016.

[53] S L Kokjohn, R M Hanson, D A Splitter, and R D Reitz. Fuel reactivity controlled compression ignition (RCCI): a pathway to controlled high-efficiency clean combustion. International Journal of Engine Research, 12(3):209–226, 2011.

[54] Chaitanya Kavuri, Jordan Paz, and Sage L Kokjohn. A comparison of Reactivity Controlled Compression Ignition (RCCI) and Gasoline Compression Ignition (GCI) strategies at high load, low speed conditions. Energy Conversion and Management, 127:324–341, 2016.

[55] Mark P B Musculus, Paul C Miles, and Lyle M Pickett. Conceptual models for partially premixed low-temperature diesel combustion. Progress in Energy and Combustion Science, 39(2–3):246–283, 2013.

[56] Development of Premixed Low-Temperature Diesel Combustion in a HSDI Diesel Engine. 2008 SAE World Congress, 2008(SP-2168):776–790, 2008.

[57] Stephen Ciatti and Swami Nathan Subramanian. An experimental investigation of low-octane gasoline in diesel engines. Journal of engineering for gas turbines and power, 133(9):92802, 2011.

[58] Gautam Tavanappa Kalghatgi. Fuel/engine interactions. 2014.

[59] A. B. Dempsey, S. J. Curran, and R. M. Wagner. A perspective on the range of gasoline compression ignition combustion strategies for high engine efficiency and low NOx and soot emissions: Effects of in-cylinder fuel stratification. International Journal of Engine Research, 1(8):1–21, 2016.

[60] Hongqiang Yang, Shijin Shuai, Zhi Wang, and Jianxin Wang. Effect of Injection Timing on PPCI and MPCI Mode Fueled With Straight-Run Naphtha. Journal of Engineering for Gas Turbines and Power, 136(3):031501, 2013.

[61] D. Kim, I. Ekoto, W.F. Colban, and P.C. Miles. In-cylinder CO and UHC Imaging in a Light-Duty Diesel Engine during PPCI Low-Temperature Combustion. SAE Int. J. Fuels Lubr., 1(1):933–956, 2008.

[62] Benjamin Petersen, Paul C Miles, and Dipankar Sahoo. Equivalence Ratio Distributions in a Light-Duty Diesel Engine Operating under Partially Premixed Conditions. SAE Int. J. Engines, 5(2):526–537, 2012.

[63] Isaac W Ekoto, William F Colban, Paul C Miles, Ulf Aronsson, Öivind Andersson, Sung Wook Park, David E Foster, and Rolf D Reitz. UHC and CO emissions sources from a light-duty diesel engine undergoing late-injection low-temperature combustion. In ASME 2009 Internal Combustion Engine Division Fall Technical Conference, pages 163–172. American Society of Mechanical Engineers, 2009.

[64] Sanghoon Kook, Choongsik Bae, Paul C Miles, Dae Choi, and Lyle M Pickett. The influence of charge dilution and injection timing on low-temperature diesel combustion and emissions. Technical report, 2005.

[65] Gautam T Kalghatgi, Per Risberg, and Hans-Erik Ångström. Advantages of Fuels with High Resistance to Auto-ignition in Late-injection, Low-temperature, Compression Ignition Combustion. 2006.

[66] Gautam T Kalghatgi, Per Risberg, and Hans-Erik Ångström. Partially Pre-Mixed Auto-Ignition of Gasoline to Attain Low Smoke and Low NOx at High Load in a Compression Ignition Engine and Comparison with a Diesel Fuel, 2007.

[67] Mark C Sellnau, James Sinnamon, Kevin Hoyer, Junghwan Kim, Marilou Cavotta, and Harry Husted. Part-Load Operation of Gasoline Direct-Injection Compression Ignition (GDCI) Engine. SAE Int. J. Engines, pages 1–24, 2013.

[68] Mark Sellnau, Matthew Foster, Kevin Hoyer, Wayne Moore, James Sinnamon, and Harry Husted. Development of a Gasoline Direct Injection Compression Ignition (GDCI) Engine. SAE Int. J. Engines, 7(2):835–851, 2014.

[69] Mark Sellnau, Wayne Moore, James Sinnamon, Kevin Hoyer, Matthew Foster, and Harry Husted. GDCI Multi-Cylinder Engine for High Fuel Efficiency and Low Emissions. SAE Int. J. Engines, 8(2):775–790, 2015.

[70] Christine Mounaim Rousselle, Fabrice Foucher, and Amine Labreche. Optimization of Gasoline Partially Premixed Combustion Mode. SAE international, (x):1–10, 2013.

[71] Amine Labreche, Fabrice Foucher, and Christine Rousselle. Impact of the Second Injection Characteristics and Dilution Effect on Gasoline Partially Premixed Combustion. SAE Technical Paper, 01(2673), 2014.

[72] Gautam T Kalghatgi, Leif Hildingsson, and Bengt Johansson. Low NOx and Low Smoke Operation of a Diesel Engine Using Gasolinelike Fuels. Journal of Engineering for Gas Turbines and Power, 132(9):092803, 2010.

[73] Mark Sellnau, James Sinnamon, Kevin Hoyer, and Harry Husted. Gasoline Direct Injection Compression Ignition (GDCI) - Diesel-like Efficiency with Low CO2 Emissions. 2011.

[74] Vittorio Manente, Bengt Johansson, Per Tunestal, Marc Sonder, and Simone Serra. Gasoline partially premixed combustion: high efficiency, low NOx and low soot by using an advanced combustion strategy and a compression ignition engine. International Journal of Vehicle Design, 59(2/3):108, 2012.

[75] Youngchul Ra, Paul Loeper, and Michael Andrie. Gasoline DICI Engine Operation in the LTC Regime Using Triple-Pulse Injection. SAE Int. J. Engines, (2012-01-1131):1109–1132, 2012.

[76] Bishwadipa Das Adhikary, Rolf D Reitz, and Stephen Ciatti. Study of In-Cylinder Combustion and Multi-Cylinder Light Duty Compression Ignition Engine Performance Using Different RON Fuels at Light Load Conditions, 2013.

[77] Chaitanya Kavuri, Satbir Singh, Sundar Rajan Krishnan, Kalyan Kumar Srinivasan, and Stephen Ciatti. Computational Analysis of Combustion of High and Low Cetane Fuels in a Compression Ignition Engine. Journal of engineering for gas turbines and power, 136(12):121506, 2014.

[78] Vittorio Manente, Bengt Johansson, and W Cannella. Gasoline partially premixed combustion, the future of internal combustion engines? International Journal of Engine Research, 12(3):194–208, 2011.

[79] Fred W Bowditch. A new tool for combustion research a quartz piston engine. SAE Technical Paper 610002, 1961.

[80] Ulf Aronsson. Processes in Optical Diesel Engines-Emissions Formation and Heat Release. PhD thesis, 2011.

[81] Günter P Merker, Christian Schwarz, and Rüdiger Teichmann. Combustion engines development: mixture formation, combustion, emissions and simulation. Springer Science & Business Media, 2011.

[82] Gerhard Woschni. A universally applicable equation for the instantaneous heat transfer coefficient in the internal combustion engine. Technical report, 1967.

[83] Alan C Eckbreth. Laser diagnostics for combustion temperature and species, volume 3. CRC Press, 1996.

[84] Hua Zhao. Laser diagnostics and optical measurement techniques in internal combustion engines. SAE International, 2012.

[85] Markus Raffel, Christian E Willert, Steve T Wereley, and Jürgen Kompenhans. Particle Image Velocimetry.

[86] Dantec Dynamics A/S. Dynamic Studio User's Guide.

[87] W F Ball, H F Pettifer, and C N F Waterhouse. Laser doppler velocimeter measurements of turbulence in a direct-injection diesel combustion chamber. In Proc Instn Mech Engrs international conference on combustion in engineering C, volume 52, pages 163–174, 1983.

[88] John Leask Lumley. The structure of inhomogeneous turbulent flows. Atmospheric turbulence and radio wave propagation, 790:166–178, 1967.

[89] L Shirovich. Turbulence and the Dynamics of Coherent Structures; Part I: Coherent Structures, Q. Appl. Math, 45:561–571, 1987.

[90] John E Dec, Wontae Hwang, and Magnus Sjöberg. An Investigation of Thermal Stratification in HCCI Engines Using Chemiluminescence Imaging, 2006.

[91] John E Dec, Yi Yang, and Nicolas Dronniou. Boosted HCCI - Controlling Pressure-Rise Rates for Performance Improvements using Partial Fuel Stratification with Conventional Gasoline. SAE Int. J. Engines, 4(1):1169–1189, 2011.

[92] Yi Yang, John E Dec, Nicolas Dronniou, and Magnus Sjöberg. Tailoring HCCI heat-release rates with partial fuel stratification: Comparison of two-stage and single-stage-ignition fuels. Proceedings of the Combustion Institute, 33(2):3047–3055, 2011.

[93] Yi Yang, John E Dec, Nicolas Dronniou, and William Cannella. Boosted HCCI Combustion Using Low-Octane Gasoline with Fully Premixed and Partially Stratified Charges. SAE Int. J. Engines, 5(3):1075–1088, 2012.

[94] Rudolf H Stanglmaier, Jianwen Li, and Ronald D Matthews. The Effect of In-Cylinder Wall Wetting Location on the HC Emissions from SI Engines. SAE Technical Paper, 1999(724), 1999.

[95] Paul C. Miles, Robert Collin, Leif Hildingsson, Anders Hultqvist, and Öivind Andersson. Combined measurements of flow structure, partially oxidized fuel, and soot in a high-speed, direct-injection diesel engine. Proceedings of the Combustion Institute, 31 II(x):2963–2970, 2007.

[96] I.W. Ekoto, W.F. Colban, P.C. Miles, U. Aronsson, ?. Andersson, S.W. Park, D.E. Foster, and R.D. Reitz. UHC and CO emissions sources from a light-duty diesel engine undergoing late-injection low-temperature combustion. Proceedings of the ASME Internal Combustion Engine Division Fall Technical Conference 2009, 2(2):411–430, 2009.

[97] Isaac W Ekoto, Will F Colban, Paul C Miles, Sungwook Park, David E Foster, and Rolf D Reitz. Sources of UHC Emissions from a Light-Duty Diesel Engine Operating in a Partially Premixed Combustion Regime. SAE Int. J. Engines, 2(1):1265–1289, 2009.

[98] TM Morel, PN Blumberg, EF Fort, and R Keribar. Methods for heat analysis and temperature field analysis of the insulated diesel. NASA CR-174783,(DOE/NASA/0342-1), 1984.

[99] F Chmela. Advanced heat transfer model for ci engines. SAE Paper, 695(1), 2005.

[100] Paul C Miles, Bret H Rempelewert, and Rolf D Reitz. Squish-Swirl and Injection-Swirl Interaction in Direct-Injection Diesel Engines.

[101] Nir Ozdor, Mark Dulger, and Eran Sher. Cyclic variability in spark ignition engines a literature survey. Technical report, 1994.

[102] Kai Liu and Daniel C Haworth. Development and Assessment of POD for Analysis of Turbulent Flow in Piston Engines. SAE Technical Paper, pages 1–6, 2011.

[103] AVL product description. Diesel Engines Thermovision Flame Image Evaluation Task. 2012.

[104] Marco Bakenhus and Rolf D Reitz. Two-Color Combustion Visualization of Single and Split Injections in a Single-Cylinder Heavy-Duty D.I. Diesel Engine Using an Endoscope-Based Imaging System. SAE Technical Paper, (724):1112–1999, 1999.

CHAPTER 7

SUMMARY OF PAPERS

Paper 1:

Combustion Stratification with Partially Premixed Combustion, PPC, Using NVO and Split Injection in a LD - Diesel Engine

Slavey Tanov[1], Robert Collin[2], Bengt Johansson[1], Martin Tunér[1]
[1] *Division of Combustion Engines, Lund University, Sweden*
[2] *Division of Combustion Physics, Lund University, Sweden*

SAE International Journal Engines 2014-01-2677

This paper presents experimental results carried out on an optical light-duty engine. A new approach to determine the fuel stratification under PPC conditions was developed. OH* chemiluminescence is used to comprehensively study the stratification level of combustion by employing different injection strategies such as single, double and triple injection together with 60 CAD negative valve overlap. Both, imaging data together with the thermodynamically data has been conducted to analyze the effects of single and multiple injections for gasoline PPC. The piston bowl was divided into 8 annular bands with a narrow width. Hence between the annular bands there is a lot distortion, therefore we look and estimate the inhomogeneity within one band, where we have less distortion. The indicate that the highest stratification level appears in the single injection case. The degree of stratification is decreasing when the injection time is advanced. This leads to a long ignition delay and hence better premixed combustion.

My contribution:

The engine and high-speed camera was performed by Robert Collin and Patrick Borgqvist before I started as a PhD student at the division. Based on the obtained engine experiments I postprocessed the data and wrote the article together with Bengt Johansson.

Paper II:

Effects of Injection Strategies on Fluid Flow and Turbulence in Partially Premixed Combustion (PPC) in a Light Duty Engine

Slavey Tanov[1], Bengt Johansson[1], Zhenkan Wang[2], Matthias Richter[2], Hua Wang[3]
[1] *Division of Combustion Engines, Lund University, Sweden*
[2] *Division of Combustion Physics, Lund University, Sweden*
[3] *Dantec Dynamics, Denmark*

SAE Technical Paper 2015-24-2455

Particle image velocimetry (PIV) measurements of the flow structure during the intake and compression were performed in the same optical engine, but without the variable valve system. At a swirl ratio of 2.6, engine speed off 800 rpm and injection pressure of 600 bar, the effects of single and multiple injection pattern on the bulk fluid motion were investigated. The vector fields were computed by using the ensemble average approach and the turbulent kinetic energy (TKE) was determined by using the cycle resolved method. We applied the ensemble averaged flow field, TKE and cycle resolved turbulence to the data with single, double and triple injection strategies including the motored case. Hence the experiments were carried out with a high-speed PIV system, the temporal turbulence level demonstrated the effects on different injection strategies. The results indicated the dominant sources of turbulence, which were found to be the fuel injection event during compression and the combustion process short after TDC. The highest turbulence level was found for single injection case, while the pilot injections for single and triple injection have shown lower turbulence levels. The turbulence level results are consistent with the stratification level results from the first paper. Higher stratification and turbulence were found for single injection, while double and triple injection cases showed lower fuel stratification and turbulence level. The key feature for that is the longer ignition delay coupled with the shorter fuel injections.

My contribution:

My part of this work was to plan and decide operating conditions, running the engine and doing the heat release calculation. Zhenkan Wang performed the PIV measurement system. The

alignment of the laser was done by Hua Wang and Zhenkan Wang and I participated to this activity in great manner. Hua Wang from Dynamic Systems supported not only with the laser system but also with correcting the highly distorted images and image post processing. Dynamic Studio was used for post processing of the raw PIV data. The obtained PIV data was then divided in two data sets, which I further postprocessed and wrote the paper together with Bengt Johansson.

Paper III:

High-Speed Particle Image Velocimetry Measurement of Partially Premixed Combustion (PPC) in a Light Duty Engine for Different Injection Strategies

Zhenkan Wang[2], Slavey Tanov[1], Bengt Johansson[1], Matthias Richter[2], Marcus Aldén[2], Hua Wang[3]
[1] *Division of Combustion Engines, Lund University, Sweden*
[2] *Division of Combustion Physics, Lund University, Sweden*
[3] *Dantec Dynamics, Denmark*

SAE Technical Paper 2015-24-2454

The sensitivity of single (2x), double(5x), triple(2x) injects were investigated under gasoline-PPC conditions. The Background for this work similar to that of the first paper. The objective was to investigate the influence of different injection strategies on in-cylinder flow field and fuel air interaction and mixing with this kind of combustion chamber design. The results indicate a clear picture of the importance of fuel injection as a turbulence generation source. It was found that injection timings earlier than -23 CAD BTDC are not forming a typical clockwise rotating vortex structure. Thus, during compression turbulence level was low because it was only depending on the bulk motion by the ascending piston. The turbulence, which plays a dominant role in transporting and mixing fuel and air, was elevated if the spray event was redirected by the piston wall.

My contribution:

My work consisted of design and planning of the operating conditions, running the engine and doing the heat release calculation. Zhenkan Wang performed the PIV measurement system. The alignment of the laser was done by Hua Wang and Zhenkan Wang and I participated to this activity in great manner. Hua Wang from Dynamic Systems supported us with laser system, correcting the highly distorted images and image post processing. Dynamic Studio was used for post processing of the raw PIV data. The obtained PIV data was then divided in two data sets, which Zhenkan further postprocessed and wrote the paper.

Paper IV:

Analyzing of In-Cylinder Flow Structures and Cyclic Variations of Partially Premix Combustion in a Light Duty Engine

Slavey Tanov[1], Bengt Johansson[1], Mohammad Izadi Najafabadi [2], Hua Wang[3]
[1] *Division of Combustion Engines, Lund University, Sweden*
[2] *Division of Combustion Technology, Eindhoven University of Technology, Netherlands*
[3] *Dantec Dynamics, Denmark*

FISITA Conference Paper F2016-ESYF-005

The motivation of this paper was to gain information not only within the piston bowl, but also in the squish region. Since multiple injections are employed, it is of great interest to gain important information about the phenomena in clearance volume during compression and late in the expansion cycle. The fluid flow in late engine cycle has a dominant role on combustion products. To determine the flow field in the piston bowl and squish region, it is crucial to operate the engine without changing the engine conditions. Therefore, the laser system was aligned two times, first focused into the piston bowl and for the second set, the camera was focused only of the squish region. Another motivation of this work was to investigate the cycle to cycle variation under PPC conditions based on the vectors fields, which was a lack in the literature. POD method is a widely tool to investigate cyclic variations. The POD decomposition technique provides a classification method based on an energy criterion by which the mean flow is seen as a superposition of coherent structures. From their temporal coefficients, it was possible to quantify its dynamical behaviour. It was seen, that the engine cycle indicated less variations until the fuel was injected, whereas the combustion induced variations were found to also significant.

My contribution:

During this work, I was hosting a visiting researcher from TU Eindhoven, Mohammad Izadi. He was responsible for the control of the PIV system with me taking some part in it. My work consisted of performing the engine runs, defining and implementing the experiment conditions to be studied, post processing of the PIV and engine data. I wrote the paper together with Bengt. Hua Wang, Mohammad Izadi and me aligned the PIV laser system and synchronized it to the engine speed. Hua Wang was responsible for image correction and in some part of the postprocessing loop.

Paper v:

Effects of Injection Timing on Fluid Flow Characteristics of Partially Premixed Combustion Based on High-Speed Particle Image Velocimetry

Mohammad Izadi Najafabadi[1], Bart Somers[1], Slavey Tanov[2], Bengt Johansson[2], Hua Wang[3]
[1] *Division of Combustion Technology, Eindhoven University of Technology, Netherlands*
[2] *Division of Combustion Engines, Lund University, Sweden*
[3] *Dantec Dynamics, Denmark*

SAE International Journal Engines 2017-01-0744

SAE International Journal Engines,2017-01-0744

This work compares single injection strategies of PPC and investigates the fluid flow characteristics. PIV measurement system was applied in a light-duty optical engine to measure fluid flow characteristics, including mean velocity and cycle-resolved turbulence, inside the piston bowl as well as the squish region with a temporal resolution of 1 crank angle degree at 800 rpm. Additionally, two injectors, having 5 and 7 holes, were compared to see their effects on fluid flow and heat release behaviour for different injection timings. Reactive and non-reactive measurements were performed to distinguish injection-driven and combustion-driven turbulence. Formation of vortices and higher turbulence levels enhance the air/fuel interaction, changing the level of fuel stratification and combustion duration. Results demonstrate clearly how turbulence level correlates with heat release behavior, and provide a quantitative dataset for validation of numerical simulations.

My contribution:

My work consisted of operating the engine and associated systems together with the Mohammad Izadi. I was also involved in making the choice of operating parameters and conditions. He was responsible for the control of the PIV system with me taking some part in it. The evaluation of the experimental data was performed by Mohammad Izadi and as well as the paper was written by him. Hua Wang, Mohammad Izadi and me aligned the PIV laser system and synchronized it to the engine speed. Hua Wang was responsible for image correction and in some part of the postprocessing loop.

Paper vi:

Influence of Spatial and Temporal Distribution of Turbulent Kinetic Energy on Partially Premixed Combustion Heat Transfer in a Light Duty

Slavey Tanov[1], Öivind Anderson[1], Leonardo Pachano2[2], Antonio García[2], José M. García-

Oliver[2], Zhenkan Wang[3],Matthias Richter[2], Marcus Aldén[2], Hua Wang[4]
[1] *Division of Combustion Engines, Lund University, Sweden*
[2] *CMT Motores Térmicos – Universitat Politècnica de València, Spain*
[3] *Division of Combustion Physics, Lund University, Sweden*
[3] *Dantec Dynamics, Denmark*

Manuscript submitted to Applied Thermal Engineering, *ATE* – 2017 – 2876.

This works is based on the PIV experimental data obtained from earlier study in 2014 (Paper 2) and deals with a new approach to comprehensively analyze spatial and temporal evolution of TKE. Since the turbulence of the bulk motion has a great influence on the mixing process and further on the combustion process, it is of great interest to develop new methodology to determine TKE. A key feature is, that the cycles for TKE are averaged along the axial direction and normalized by maximum TKE in order to allow a more direct comparison of TKE spatial evolution under firing conditions. In addition, this paper aims to gain an insight into convective wall heat transfer coefficient heat transfer coefficient which plays a dominant role on combustion and emission process. In this paper the heat transfer coefficients were derived from the experimental PIV data, where radial and axial components of velocity used. There was a strong correlation between TKE spatial and temporal evolution and heat transfer. High TKE levels introduce peak values into the heat transfer coefficient temporal evolution.

My contribution:

The PIV measurements were performed by me and Zhenkan Wang and I operated the engine as well as taking care of heat release analysis. Leonardo Pachano was responsible for the PIV postprocessing and the paper was written by him and me.

Paper VII:

Combustion and Emission Characteristics of Gasoline-PPC with small quantities of Ethanol

Slavey Tanov[1], Öivind Anderson[1], Khanh Cung[2], Stephen Ciatti[2]
[1] *Division of Combustion Engines, Lund University, Sweden*
[2] *Argonne National Laboratory, USA*

To be submitted to a journal

The combustion and emission characteristics of gasoline fuel with quantities of ethanol content (30 vol.%, having significantly influence on soot formation, are investigated in a

stock engine over a range of EGR and λ levels. The addition of ethanol to gasoline results in an increase in octane number, which is feasible for PPC operation. Higher octane number enables a longer premixing of fuel and air prior to auto-ignition. The results demonstrate close to smokeless combustion for all measurement points. The thermal NO_x formation was suppressed as a result of cooled EGR, which decreases the combustion temperature. In addition, the engine was fitted with an endoscope for visualization of the combustion sequence and to detect soot formation. The endoscopic images demonstrate a smokeless combustion for $\lambda = 1.8$ operation with 20%EGR.

My contribution:

The PIV measurements were performed by me and Zhenkan Wang and I operated the engine as well as taking care of heat release analysis. Leonardo Pachano was responsible for the PIV postprocessing and the paper was written by him and me.